NASA Technical Paper 1625

Parametric Study of Variation in Cargo-Airplane Performance Related to Progression From Current to Spanloader Designs

Thomas A. Toll

APRIL 1980

NASA

NASA Technical Paper 1625

Parametric Study of Variation in Cargo-Airplane Performance Related to Progression From Current to Spanloader Designs

Thomas A. Toll
Langley Research Center
Hampton, Virginia

i

SUMMARY

A parametric analysis has been made to investigate the relationship between cur-
rent cargo airplanes and possible future designs that may differ greatly in both size and
configuration. This analysis applies empirical scaling laws developed from statistical
studies of data from current and advanced-study airplanes and, in addition, accounts for
payload density, effects of span-distributed load, and variations in tail-area ratio. The
method is believed to be particularly useful for exploratory studies of design and tech-
nology options for large airplanes.

The analysis predicts somewhat more favorable variations of the ratios of payload
to gross weight and block fuel to payload as the airplane size is increased than has been
generally understood from interpretations of the cube-square law. In terms of these
same ratios, large all-wing (spanloader) designs show an advantage over wing-fuselage
designs; however, the comparison could be modified by other considerations.

INTRODUCTION

In comparison with the various surface-transportation modes, air transportation
still seems to be far from a settled state, as is evidenced by its continued growth in
popularity and the diversity of its operations. Improvements in efficiency, in terms of
cost and time, have tended to generate new business and to attract some transfer from
other modes. One important restraint to the rate of growth of the air mode stems from
problems of providing facilities for ground and airways control. This restraint is
related more to the numbers of aircraft than to the quantity of goods handled. Because
of this consideration, as well as the desire to minimize the total personnel in flight
crews, continued growth in size of aircraft deserves careful consideration as a potential
course for the future.

The question of whether there is a limit to airplane size, in terms of either dimen-
sions or weight, beyond which thoughts of continued growth cannot profitably be pursued
has been debated throughout the history of manned aircraft. Specific limits have been
suggested in the past; however, these limits have been exceeded by one means or another
as airplanes have continued to grow until a gross weight of 4.45 MN $(1 \times 10^6$ lb) is near
reality for airplanes in service (Boeing 747 and Lockheed C-5A). For even larger air-
planes, volume in the wing becomes increasingly available for carrying payload, until

eventually the fuselage becomes unnecessary, provided the nature of the payload is such that it can be accommodated in the space in the wing.

An interesting consequence of such limiting concepts results from distribution of weight along the wing span and the associated reduction in bending stress; thus, the descriptive name "spanloader" is being applied to these all-wing airplanes. Recent industry and NASA studies have indicated attractive possibilities for these designs, with gross weights in the range from 6.67 MN to 17.79 MN (1.5×10^6 lb to 4.0×10^6 lb). (See refs. 1 to 5.)

The present study uses a parametric scaling method as a means of exploring the relationship between conventional wing-fuselage and all-wing concepts. A modification of the Boeing 747 freighter is used as a baseline configuration in the scaling study. Results obtained by scaling to a limiting (all-wing) condition are compared with data from a representative spanloader study airplane from reference 4. Scaling laws for the primary airplane weight groups were derived from statistical studies of data for large aircraft ranging from those in the current fleet to advanced design studies. An equation is developed for approximating wing weight in terms of geometric parameters, load-distribution effects, and the level of structural technology. The calculated results contribute to an understanding of the progression from conventional to spanloader designs by indicating trends of certain performance parameters and by showing effects of variations in design conditions, such as wing loading and payload density. The method applied herein is considered to be useful for exploratory studies of innovative designs, for establishing parametric ranges in contractor studies of advanced designs, and for evaluating effects of advanced technologies.

Use of trade names or names of manufacturers in this report does not constitute an official endorsement of such products or manufacturers, either expressed or implied, by the National Aeronautics and Space Administration.

SYMBOLS

Values are given in SI units with U.S. Customary Units in parentheses. Measurements and calculations were made in U.S. Customary Units.

A   aspect ratio

D_{PL} payload density (payload weight divided by total volume potentially available for payload)

I_B correlation index for wing weight for resisting bending moment

I_M correlation index for wing weight for resisting miscellaneous loads (other than bending moment)

K_A aerodynamic correction for determining required fuel

K_{LD} load-distribution relief factor

K_{ST} structural-technology factor

L linear scale factor

L/D lift-drag ratio

n scaling exponent, applied to linear scale factor

n' scaling exponent, applied to wing reference area $\left(n' = \frac{1}{2}n\right)$

R range, km   (n. mi.)

S reference area of aerodynamic surface

SFC specific fuel consumption

t/c wing-section thickness ratio

U airplane ultimate load factor (assumed equal to 3.75 for cargo airplanes)

$\overline{V}$ volume as defined by external dimensions of fuselage and wing

W weight, N   (lb)

W_G take-off gross weight, N   (lb)

W_{OE} operating (empty) weight, N   (lb)

λ wing taper ratio

$\Lambda_{c/4}$ wing quarter-chord sweep angle, deg

Subscripts:

B	body
E	equipment
F	total fuel
F,B	block fuel
F,R	reserve fuel
L	landing gear
Fl	flight
Gr	ground
max	maximum
P	propulsion (engines, pylons, nacelles)
PL	payload
S	structure
T	tail
U	useful load
W	wing
ZF	zero fuel

BACKGROUND – "THE CUBE-SQUARE LAW"

There is little merit in attempting a discussion of trends in aircraft characteristics as size is increased without recognizing the cube-square concept, which has provided the basis for much of the discussion and controversy on size projections in the past. An

4

excellent discussion of the general area of size scaling, including many of the implications and limitations of the cube-square law, is given in reference 6. Some additional discussions of the law in relation to various analytical objectives are given in references 5, 7, and 8. The present study makes use of extensions of the cube-square law that were developed in reference 8 and adds some additional refinements and interpretations.

In its simplest form, the cube-square law specifies that volume varies as linear scale cubed, and representative areas vary as linear scale squared for structural members of varying size, but of similar shape, and composed of solid homogeneous (constant density) material. When the aerodynamic load is assumed to be equal to the material volume – which is approximately true for birds – a consequence of the law is that wing loading and material stress both increase in proportion to the scale. Although these relations are of some interest for aircraft (see refs. 6 and 7), a more useful application is to hollow, rather than solid, structures, which allows imposition of a condition of constant wing loading. Now, if geometric similarity and constant unit stress are assumed, the law again indicates that for a simple bending-load condition, material weight increases as the linear scale cubed, and therefore structural weight divided by a representative surface area increases in proportion to the linear scale. This latter interpretation of the cube-square law is useful in considering size projections, provided limitations, such as the following, are appreciated:

(1) Aircraft are subjected to many different loads, some of which vary with scale at a lesser rate than simple bending; therefore, the overall weight growth also increases with size at a somewhat lower rate than predicted by the cube-square law.

(2) Improvements in technology have come about concurrently with the evolutionary growth in airplane size. This development has had the effect of avoiding the increase in structural weight fractions that might otherwise have occurred.

(3) Large airplanes usually are proportioned differently from small airplanes, since simple geometric scaling causes volume to be generated faster than it can be used efficiently for a given kind of payload. By adjusting the size of the payload vessel (usually the fuselage) to satisfy a constant payload density, the size of the vessel becomes smaller (relatively) and lighter than is indicated by geometric scaling. This characteristic of real aircraft is consistent with the cube-square law when applied separately to major components (wings and bodies) instead of to the airplane as a unit.

Additional remarks on the significance of the cube-square law in relation to results generated in the present study are made as a part of the subsequent discussion.

METHOD OF ANALYSIS

Reference Aircraft

Plan views are shown in figure 1 for two freighter configurations, one representing current design practice, and the second representing a spanloader design, which has been shown by recent studies to have attractive possibilities for the 1995 to 2000 time period. Both drawings are to the same scale, the conventional or "baseline" airplane used in the subsequent analytical study being of the size and configuration of the Boeing 747-200F although differing in technology level. The differences between the two reference aircraft of figure 1 — in size and appearance — are indeed very great. The baseline airplane was derived from the Boeing 747-200F by applying levels of technology advances as determined by contractor studies carried out under the NASA Advanced Transport Technology (ATT) program. (See refs. 9 to 11.) The selected advanced technology conversion factors are given in table I and also the resulting group weights for the baseline airplane. The improvements permitted a reduction in empty weight and fuel and, consequently, an increase in payload, whereas the gross weight and cruise Mach number are held at the values for the Boeing 747-200F. Pertinent quantitative information for the baseline airplane and the spanloader (Boeing 759-211) are compared in figure 1. The fact that the wing loading of the spanloader is half that of the baseline is especially significant. The low wing loading allows the spanloader to take off and land with no rotation and with relatively simple lift flaps, and it also allows the necessary volume in the wing for payload at a not unreasonable gross weight. The design range of both reference airplanes is indicated to be 5556 km (3000 n. mi.), which was determined by fuel/payload adjustments from available specification data, that is, from a range of 5334 km (2880 n. mi.) for the Boeing 747-200F and 6668 km (3600 n. mi.) for the spanloader.

Figure 2 shows comparisons of the two reference airplanes in terms of gross weight W_G, wing loading W_G/S_W, and two convenient performance yardsticks that will be used repeatedly in the present study — that is, the ratio of payload to gross weight W_{PL}/W_G and the ratio of block fuel to payload $W_{F,B}/W_{PL}$. The improvements in the performance yardsticks brought about by application of advanced technologies in adjusting the Boeing 747-200F to the baseline reference airplane are substantial; however, the resulting values still are very inferior to those of the spanloader. The analysis to be presented develops the variation of these yardsticks through a progression from the baseline to an all-wing, or spanloader configuration and should thereby provide indications of characteristics expected for intermediate-size aircraft. The procedure used in performing the calculations is described.

Calculation Procedure

The method used for the calculations is discussed only in a general sense; however, the description given is believed to be sufficient to provide an understanding of the basis for results described later in the paper, and it also should be adequate as a guide to individuals having some background in the disciplines of airplane design for applying the method to other problems.

The object of the method is derivation of valid trends of various performance parameters and of associated variations in the relative sizes of fuselage and wing by scaling from a suitable baseline airplane. The baseline should be a developed airplane, or at least a design that has received enough attention to give reasonable assurance that the various performance and operating specifications can be realized. The approach of limiting calculations to trends from a baseline permits useful results to be obtained even though the various disciplinary inputs are less exact or detailed than is necessary in performing preliminary point designs while starting from base zero for the inputs. Also, by imposing certain restraints – such as wing geometry, thrust-weight ratio, and cruise speed – it can be shown that aircraft derived by scaling will satisfy, to a first order, many of the specifications (for example, takeoff and climb) that were satisfied by the baseline. It is emphasized that the intended use of the method is primarily for exploratory studies and for providing a better understanding of the basis for changes in characteristics that are a consequence of parametric variations. When these objectives are considered, there is an advantage in limiting the number of inputs in the calculation process to the minimum necessary for preserving reasonable validity of calculated results.

After defining the dimensions, weights, and performance of a suitable baseline, a matrix of configurations is developed to represent systematic variations from the baseline, as shown in figure 3. The wings of the airplanes in the matrix all are of similar shape, as is also true of the fuselages (constant fineness ratio). In each horizontal sequence, the wings are of constant area, whereas the fuselage size decreases in going from left to right. The longitudinal location of tail surfaces is not assumed to be constrained by the fuselage length. Each vertical sequence represents a variation in airplane scale, while the relative sizes of fuselage and wing remain unchanged. Although only three sketches are shown in figure 3 for each vertical sequence, calculations for four to six sizes – each identified by a specific value of the linear scale factor L – ordinarily are made.

A specific value for the nondimensional shape parameter $\overline{V}^{2/3}/S_W$ can be related to all airplanes of a vertical sequence. The symbol $\overline{V}$ denotes the combined volume of wing and fuselage, based on external dimensions, and S_W is the reference area of the wing. A limiting value of the shape parameter is obtained when the fuselage volume is

7

reduced to zero. As sketched in figure 3, in which the indicated tail length approximates that of tip controls for all-wing aircraft, these limiting configurations are unrealistic, since no structural support remains for the center-mounted tail. Adjustments to the more reasonable spanloader design, which uses tip-mounted fins, are made in the course of the subsequent analysis.

Two tail-geometry series are indicated in figure 3, one for which the ratio of tail area to wing area remains constant at $S_T/S_W = 0.36$ and one in which S_T/S_W varies from 0.36 for the baseline to 0.13 for the airplane with zero-volume fuselage. The latter value is approximately equal to that for the spanloader, where S_T is interpreted as the total planform area for the wing-tip fins. Figure 4(a) shows plots of S_T/S_W against $\overline{V}^{2/3}/S_W$ for the two tail-geometry series. The subsequent analysis includes an evaluation of the effect of the two tail-geometry series on payload and fuel yardsticks.

Figure 4(a) also shows assumed values of the load-distribution relief factor K_{LD}, which appears in the wing-weight equation developed in the appendix. For one condition, K_{LD} remains constant at the baseline value (0.8), and for a second condition, K_{LD} varies linearly from the baseline value to 0.3 when the fuselage has vanished. The rationale for the latter condition is described in the appendix and stems from reduced suspended weight at the plane of symmetry as fuselage size (relative to wing size) is reduced. The subsequent analysis includes a comparison of effects on performance yardsticks of the two assumptions for K_{LD}.

While holding each specific value of $\overline{V}^{2/3}/S_W$ constant, size is varied by application of different values of the scale factor L. Obviously, for geometric scaling, the following relations are exact:

Representative length $\propto L$

Representative surface area $\propto L^2$

Representative volume $\propto L^3$

Component structural weights bear a more subtle relationship to the scale factor because of their dependence on loading conditions, including both the wing-loading parameter W_G/S_W and the load distribution. With W_G/S_W held constant but with no consideration of load distribution, the simple cube-square concept suggests that for the wing, fuselage, or tail,

Component weight $\propto L^3$

However, under real-life conditions in which load distribution is considered, the weight-scaling relation must be written as

$$\text{Component weight} \propto L^n$$

Values of the exponent n have been determined for different weight groups by correlation of data available from current airplanes and from industry design studies. The values determined are listed in table II along with corresponding values suggested by the simple cube-square concept. Table II also shows typical component group weights as fractions of airplane gross weight for conventional and spanloader designs. Obviously, the scaling laws associated with component weight groups having large weight fractions need to be determined more accurately than those with smaller weight fractions. The wing is of primary importance for both airplane types, and the fuselage is about equal to the wing for conventional designs. Other weight groups that make up the operating (empty) weight are less important since they have fractions about one-half, or less, as large as the wing.

The total fuel carried in an airplane is the sum of the block fuel $W_{F,B}$ and the reserve fuel $W_{F,R}$. In design studies, reserve fuel must be calculated in accordance with Federal Air Regulations that specify provisions for loiter time and flight to an alternate base. For the parametric study, in which range is held constant, reserve fuel is approximated as always being the same percentage of block fuel as is given for the baseline airplane in figure 1.

The block fuel required by airplanes scaled from the baseline, while range and wing loading are held constant, can be written as

$$\text{Scaled } W_{F,B} \quad \left(\text{Baseline } W_{F,B}\right) L^2 K_A$$

where L^2 corrects for changes in gross weight and K_A is a correction for any change in aerodynamic efficiency, such as may result from the skin-friction coefficients and ratios of wetted area to wing area. The correction K_A can be calculated from the Breguet range formula as the ratio of the fuel required by a scaled airplane to that required by the baseline for the same block distance and gross weight. With velocity and SFC constant, an acceptable approximation to the correction is simply

$$K_A = \frac{\text{Baseline } (L/D)_{max}}{\text{Scaled } (L/D)_{max}}$$

Values for $(L/D)_{max}$ can be determined from one of the several methods used in preliminary design, in which skin-friction coefficients of the wing and fuselage are evaluated separately at the appropriate Reynolds number for each. For the results presented herein, all-turbulent flow conditions were assumed in evaluating skin-friction coefficients. After having calculated the operating weight and the total fuel weight for any given combination of $\overline{V}^{2/3}/S_W$ and L, the corresponding payload weight is obtained from

$$W_{PL} = W_G - W_{OE} - W_F$$

The next step involves determination of the volume available in the aircraft for useful load (fuel plus payload) after requirements for structure, systems, and flight crew have been satisfied. A review of several transport airplane designs suggests that for medium and long-range transports, about 65 percent of the fuselage volume (based on external dimensions) is potentially available for fuel plus payload, even though a considerably smaller percentage normally is used by freighter-type airplanes. The available volume in the wing depends on wing area, thickness ratio, and profile; however, for the conditions of this study, a variation from 40 percent of the total volume for a wing of 464 m^2 (5000 ft^2) to about 55 percent for a wing area of 3716 m^2 (40 000 ft^2) has been determined and is plotted in figure 4(b). Volume available for payload is obtained as the difference between the total volume available for useful load and that required by the fuel system (fuel, tanks, and plumbing). The total volume $\overline{V}_F$ required to accommodate the fuel system is estimated to be about 1.2 times the volume of the fuel itself. The volume available for payload is now calculated from the relation

$$\overline{V}_{PL} = \overline{V}_U - \overline{V}_F$$

A nominal value of the payload density, which corresponds to the assumptions described, is given by

$$D_{PL} = \frac{W_{PL}}{\overline{V}_{PL}}$$

The values so calculated can be very different from values quoted in other studies for payload density that may have a different basis, such as that of containerized cargo. Nevertheless, a nominal-density basis is very useful in exploratory studies, since it refers to a potential (or near optimum) capability without restraints that are not necessarily permanent, such as the dimensions of the payload containers and floor height. After generalized results based on the nominal condition have been calculated, conversion to specific

10

airplanes with fixed constraints can be accomplished, but this conversion is not described in this paper.

Curves of D_{PL}, calculated in the manner described, can be plotted against gross weight — determined by variations of the linear scale factor L — for each of the several values of $\overline{V}^{2/3}/S_W$ given in figure 3. A set of such curves is given in figure 5 and represents the basic payload condition for the present study; that is, the payload is of a bulk nature and can occupy available volume in either the fuselage or the wing. A comparable set of curves can as easily be made for the condition of the payload restricted to volume available only in the fuselage. A comparison of the two conditions, in terms of the performance yardsticks, is made later in the paper. Other conditions for the data of figure 5 are wing loading equal to that of the baseline airplane, variable tail-area ratio and variable load-distribution relief as given by the solid curves of figure 4, and scaling laws from the semiempirical column of table II, but with wing weight defined by the general equation of the appendix. A point representing the payload density of the baseline airplane is shown in figure 5. A horizontal line drawn through this point provides intersections that define values of gross weight W_G, corresponding to each of the prescribed values of $\overline{V}^{2/3}/S_W$ at the baseline payload density of 109 kg/m^3 (6.8 lb/ft^3). These intersections can be applied to plots of the performance yardsticks W_{PL}/W_G and $W_{F,B}/W_{PL}$ to determine variations of these parameters with gross weight at the value of the payload density for the baseline airplane. Similar sets of intersections, corresponding to other constant values of D_{PL}, can be obtained from other horizontal lines at selected levels in figure 5 and used to obtain curves of the performance yardsticks for the additional values of D_{PL}. Such results are presented in the section "Results and Discussion."

As previously noted, the approximations made in the calculations are considered to be justified by the fact that the objective is to establish trends in characteristics from a baseline airplane. The performance parameters are determined without giving consideration to the individual segments of a design flight profile, that is, take-off, climb, cruise, descent, and landing. When it has been necessary to determine the fuel required to cover the design range, reliance has been placed on results from more detailed studies in which the profile segments were considered. These results led to the approximation that for medium- and long-range subsonic transports, the actual fuel used from start of take-off to landing is very nearly equal to that calculated from the Breguet range formula for a range about 370 km (200 n. mi.) longer than the design range. For the present study, this correction was applied only in adjusting data for the reference airplanes from that given in available specifications, in which the design range differed moderately from the desired study value, to the study value for both airplanes, $R = 5556$ km (3000 n. mi.)

No attempt is made in the present study to match aircraft aerodynamics with specific engine characteristics. Since the study is aimed primarily at a distant time period (year 2000+), little is known of the characteristics of engines that may be available in that period. The assumptions made in this regard are generally in line with recent studies by industry of advanced airplane concepts. In the present study it is assumed that for a given design wing loading W_G/S_W, all airplanes scaled from the baseline will operate at their respective values of $(L/D)_{max}$ at the conditions determined to be optimum for the baseline at the midpoint of its design range; that is, the Mach number, altitude, and specific fuel consumption are the same as those for the baseline design condition. An error results from the fact that the lift coefficient for $(L/D)_{max}$, and hence the altitude, actually vary as airplane size (Reynolds number) and $\overline{V}^{2/3}/S_W$ are changed. Therefore, neither the operating L/D nor the engine efficiency are always at the optimum values; however, the resulting error in the variation of block fuel from the baseline value is expected to be less than 5 percent.

Another assumption is that the allowable take-off distance imposes the critical requirement on engine thrust; therefore, since the wing planform does not change, the thrust-weight ratio must remain essentially constant for the different configurations, even though cruise L/D may change significantly over the range of scaled conditions. This assumption is admittedly crude; however, it is not especially significant, since the maximum error in weight could hardly be more than one-fifth of the total propulsion-system weight, or a little more than 1 percent of the airplane gross weight.

OUTLINE OF PRESENTED RESULTS

Most of the calculated data to be presented in the section "Results and Discussion" consist of variations against airplane gross weight of the ratio of payload to gross weight W_{PL}/W_G and the ratio of block fuel to payload $W_{F,B}/W_{PL}$ for selected constant values of the shape parameter $\overline{V}^{2/3}/S_W$, the payload density D_{PL}, and the wing loading W_G/S_W. Four sections are used, with titles and associated figures as follows:

12

The first section presents trends in the performance yardsticks brought about by scaling from the baseline airplane. While wing loading is maintained at the baseline value, wing weight is calculated from the general equation developed in the appendix, payload is located in available volume of both fuselage and wing, and both load-distribution relief and tail-area ratio vary with $\overline{V}^{2/3}/S_W$ in accordance with the solid lines of figure 4(a).

The second section shows sensitivities of the calculated results to variations from the conditions selected for the first section. These variations include (1) calculation of wing weight from the simple cube-square law and from a semiempirical law rather than from the general equation, (2) restricting the payload location to the fuselage, and (3) keeping both the load-distribution relief and the tail-area ratio independent of $\overline{V}^{2/3}/S_W$. The wing loading is held constant at the baseline value for all the results presented.

The third section shows the effect of reducing wing loading in two steps from that of the baseline to that of the spanloader and of extending the results to airplane sizes that permit reduction of the fuselage volume to zero and carrying the entire payload in the wing. Aside from the wing loading variation, all conditions for this section are identical with those of the first section.

The fourth section summarizes calculated results pertinent to the progression of characteristics from the baseline airplane to the spanloader and includes some additional observations of a general nature.

RESULTS AND DISCUSSION

Scaled Baseline Data Matrix

Several variations of assumed conditions are considered in the course of the present discussion; however, an initial data matrix is developed to represent a best estimate of the consequence of varying the size (volume) of conventional freighter aircraft designed to carry bulk cargo in volume that is available in both the fuselage and the wing and having the wing loading of the baseline airplane. Load-distribution relief and tail-area ratio are assumed to be dependent on the shape parameter $\overline{V}^{2/3}/S_W$ in accordance with the solid lines shown in figure 4. The scaling laws used in the calculations are those given in the column labeled "Semiempirical" in table II, but with wing weight determined from the general equation developed in the appendix.

Calculated results for the payload ratio W_{PL}/W_G are shown in figure 6. The dashed lines represent variations for constant values of the shape parameter $\overline{V}^{2/3}/S_W$, and therefore indicate the effect of simple geometric scaling with no change in shape.

13

The solid lines apply to constant values of the payload density D_{PL} and were constructed by use of the intersections of the constant $\overline{V}^{2/3}/S_W$ curves from figure 5. The dashed lines of figure 6 show decreasing values of W_{PL}/W_G as gross weight is increased. The rate of decrease ranges from gradual to rather rapid as $\overline{V}^{2/3}/S_W$ advances from its minimum value (no fuselage) to its maximum value (largest fuselage). This unpromising indication of the outlook for very large airplanes corresponds to an interpretation of the cube-square law sometimes cited in early aviation history as evidence of an economic limitation to the size of aircraft. Further consideration leads to the finding, however, that the volume available for payload increases more rapidly than is required for a payload of constant density. The solid lines of figure 6 show that when fuselage size is adjusted to that required for constant payload density, the payload ratio increases with gross weight, particularly over the range of W_G up to 8.90 MN $(2 \times 10^6$ lb). The progressive change in relative size of the fuselage and wing when W_G is increased while D_{PL} is constant can be visualized by noting in figure 3 the configurations corresponding to values of $\overline{V}^{2/3}/S_W$ traversed by the constant D_{PL} lines of figure 6.

Comparison of results for constant D_{PL} with results for constant $\overline{V}^{2/3}/S_W$ in figure 6 illustrates the effect of applying scaling laws separately to the wing and to the fuselage, with relative sizes determined by the nature of the payload, rather than applying scaling laws to the complete airplane as a unit. Because of the high wing-loading condition of figure 6, projection of the results to all-wing designs $\left(\text{zero-volume fuselage, or } \overline{V}^{2/3}/S_W = 0.117\right)$ would indicate viable aircraft only for very high payload densities $\left(D_{PL} > 320 \text{ kg/m}^3 \text{ (20 lb/ft}^3)\right)$ or for gross weights beyond 17.79 MN $(4 \times 10^6$ lb).

Results presented in figure 6 and throughout the paper do not account for a minimum material thickness gage that is normally available. Although this effect may be significant at the low portion of the W_G scale and may cause the indicated trend of W_{PL}/W_G to be optimistic at low W_G, the effect is not believed to be important at the higher W_G values, which are of most interest in this study. Also, at this time, one can only speculate on probable minimum gage values for composite materials that are expected to be widely used by the year 2000.

Results for block-fuel ratio $W_{F,B}/W_{PL}$ for the conditions of figure 6 are presented in figure 7. Quite a rapid improvement in block-fuel ratio is shown for constant values of D_{PL} as W_G is increased over the range to about 8.90 MN $(2 \times 10^6$ lb). Some of the improvement should be expected from the gains in payload ratio noted previously, since such gains indicate less airplane weight per unit weight of payload. A

greater part of the improvement, however, is brought about by increased aerodynamic efficiency, $(L/D)_{max}$ variation with W_G, as shown in figure 8. The relatively small increase in $(L/D)_{max}$ with W_G when $\overline{V}^{2/3}/S_W$ is held constant results simply from the effect of Reynolds number in reducing the turbulent skin-friction coefficient. The differences between the curves for constant D_{PL} and the curves for constant $\overline{V}^{2/3}/S_W$ result from the changing proportions of fuselage and wing sizes and thereby change the ratio of total airplane wetted area to wing planform reference area. For an increase in W_G from 0.89 MN (2×10^5 lb) to 8.90 MN (2×10^6 lb), the overall $(L/D)_{max}$ improvement is 29 percent, whereas the improvement in fuel-to-payload ratio over the same range is 33 percent.

Indications of the sensitivities of calculated results to each of the conditions selected for figures 6 to 8 are described in the following section. The material is not essential to the primary object of scaling from the baseline airplane to a spanloader.

Sensitivities to Scaling Laws, Location of Payload, Load-Distribution Relief, and Tail-Area Ratio

The sensitivity of the calculated payload ratio W_{PL}/W_G to specific weight-scaling laws is shown in figure 9. Results are given for three scaling scenarios: one scenario uses scaling exponents from the simple cube-square concept (table II); a second uses the semiempirical exponents given in table II; and a third uses the semiempirical scaling exponents for the fuselage and tail while wing weight is calculated from the general equation of the appendix. The third scenario is the same as that used in figures 6 to 8. For each scenario, two data curves are given: one corresponds to the configuration of the baseline airplane $\left(\overline{V}^{2/3}/S_W = 0.34\right)$ but with D_{PL} permitted to vary, and the second represents constant payload density at the baseline value of $D_{PL} = 109$ kg/m^3 (6.8 lb/ft^3) while the configuration is permitted to vary.

Results given in figure 9 for the payload ratio are found to be very sensitive to the change in value of the scaling exponents regardless of whether configuration or payload density is held constant. Nevertheless, when fuselage size is adjusted to maintain constant D_{PL} as W_G is increased, the payload ratio does not appear to decrease even when the scaling exponents from the simple cube-square concept are used. It is also noted that results obtained by using all semiempirical exponents are almost identical with results obtained when the general wing-weight equation is used instead of the semiempirical scaling equation for wing weight. The general equation is required, of course, whenever it is desired to make changes in wing shape or wing loading. Results calculated for the block-fuel ratio (fig. 10) are affected by the various scaling scenarios in much the same way as the results described for the payload ratio.

Sensitivities to some additional analytical assumptions are shown in figures 11 and 12. None of the variations considered have any significant effect on curves for constant $\overline{V}^{2/3}/S_W$, and therefore, only a single curve is shown for that condition. When D_{PL} is constant, the lowest level of W_{PL}/W_G is obtained when payload is assigned only to volume available in the fuselage, when no advantage is assumed for load-distribution relief $\left(K_{LD} = 0.8\right)$, and when the ratio of tail area to wing area is constant at the value for the baseline airplane $\left(S_T/S_W = 0.36\right)$. Some improvement results when the payload can be assigned to available volume in both the fuselage and the wing while other conditions remain unchanged. A slightly larger effect on W_{PL}/W_G is obtained when advantage is taken of load-distribution relief to the extent shown by the variation given for K_{LD} in figure 4. Only a small additional advantage is obtained by permitting the tail-area ratio $\left(S_T/S_W\right)$ to vary as shown in figure 4. Sensitivities of $W_{F,B}/W_{PL}$ (fig. 12) to the same series of assumptions are generally similar to those just described for payload ratio; however, making use of available wing volume appears to be somewhat more important than was shown for the payload ratio in figure 11.

For all the results presented up to this point, the wing loading of the baseline airplane has been maintained; that is, $W_G/S_W = 6751$ N/m^2 (141 lb/ft^2). The result of reducing W_G/S_W to approach that of the reference spanloader is discussed in the next section.

Reduction of Wing Loading

Payload and block-fuel ratios are plotted against gross weight in figures 13 and 14. Note that the W_G scale covers a much larger range than that used in previous figures. Results are given for wing loadings of 4788 N/m^2 (100 lb/ft^2) and 3352 N/m^2 (70 lb/ft^2) in addition to the baseline value. For the additional values of wing loading, wing weights were calculated by the general equation from the appendix; tail weights were assumed to vary as the square root of wing loading; and fuselage weights were assumed to have the same relation to fuselage size that was used for the baseline condition.

Curves are shown in figures 13 and 14 for the baseline configuration $\left(\overline{V}^{2/3}/S_W = 0.34\right)$ and for zero-volume fuselage $\left(\overline{V}^{2/3}/S_W = 0.117\right)$. Also shown are variable-configuration curves representing constant (baseline) values of payload density $D_{PL} = 109$ kg/m^3 (6.8 lb/ft^3). Intersections of constant D_{PL} curves with the zero-fuselage curves indicate the gross weights for which all-wing (or zero-fuselage) aircraft are viable for the selected values of D_{PL} and W_G/S_W. In the context of the present exploratory study, viable aircraft are indicated at W_G slightly greater than 17.79 MN (4 × 10^6 lb) when $W_G/S_W = 3352$ N/m^2 (70 lb/ft^2) and at W_G of about 47.71 MN (10.5 × 10^6 lb) when $W_G/S_W = 4788$ N/m^2 (100 lb/ft^2). For the baseline wing loading, $W_G/S_W = 6751$ N/m^2 (141 lb/ft^2), viable all-wing aircraft would exist only at gross

16

weights far beyond the limit of the W_G scale shown in figures 13 and 14. Results indicated at the high end of the gross weight scale are, of course, highly speculative, since they correspond to sizes far beyond the range of experience, or even of serious study; nevertheless, the results shown are thought to be helpful in developing the perspective of the present study.

It should be recalled that all the present analysis is constrained to aircraft designed for a cruise Mach number of 0.85. Had a lower cruise Mach number been chosen, wings of greater thickness, and consequently of greater volume, would have been acceptable. Viable all-wing aircraft, therefore, would be indicated at lower gross weights than are indicated herein. (For example, see ref. 12.)

The results in figures 13 and 14 show that for wing-fuselage configurations with D_{PL} constant, both the payload ratio and the block-fuel ratio become more favorable as the wing loading is reduced from the baseline value. It is found from additional calculations (not presented) that the indicated effect on payload ratio is associated largely with the imposed condition that the payload occupies the volume available in both fuselage and wing. When the payload is restricted to volume available only in the fuselage, decreases in wing loading have a slightly adverse effect on the payload ratio; however, the effect on block-fuel ratio is not significantly changed from the original condition.

More complete sets of calculated results are shown in figures 15 and 16 for W_G/S_W = 3352 N/m^2 (70 lb/ft^2), which is essentially the same as the value W_G/S_W = 3323 N/m^2 (69.45 lb/ft^2) given in figure 1 for the Boeing 759-211 spanloader. Curves for D_{PL} = 136 kg/m^3 (8.5 lb/ft^3), which were calculated for the Boeing spanloader, have been included in figures 15 and 16. The significant result shown in these figures is that the intersections of the D_{PL} = 136 kg/m^3 (8.5 lb/ft^3) curves with the zero-fuselage curves are close to the specific points, in terms of W_G, W_{PL}/W_G, and $W_{F,B}/W_{PL}$ which apply to the Boeing spanloader. Therefore, the scaling process used in the analysis seems to have been reasonably reliable in tracing the progression from a conventional design to a spanloader. Some differences still remain, however, between the derived airplane and the reference spanloader.

Values for a number of weight and performance quantities for the derived all-wing airplane (to be referred to as "Baseline extrapolation") are listed in table III. Pertinent nondimensional quantities are given in figure 1. Adjustments are made for the primary differences, which are considered to be lift-drag ratio, wing geometry, and reserve fuel. No attempt has been made to explain the difference in L/D between the baseline extrapolation and the Boeing spanloader; instead, the value calculated for the baseline extrapolation (L/D = 24.4) was simply adjusted downward to the value (L/D = 21.7) given in reference 4 for the spanloader. The several differences in wing geometry have been

accounted for in a recalculation of wing weight by using the general equation from the appendix. Reserve fuel also was adjusted to the same fraction of block fuel as is shown for the Boeing spanloader, since it is quite obvious that considerably different bases for establishing reserve fuel were followed for the Boeing 747-200F and for the spanloader airplanes. The combined result of the adjustments are shown in table III under the heading "Adjusted baseline extrapolation." The adjustments do bring the airplane defined by scaling from the baseline into somewhat closer agreement with the Boeing spanloader for the quantities listed, although the effect is small compared with other steps in the scaling process. The close agreement between the derived airplane and the reference spanloader is believed to contribute to the credibility of results calculated by the scaling process.

Summary Results and Observations

In the section entitled "Reference Aircraft," comparisons in terms of size, configuration, and values of the payload and block-fuel ratios were shown for the baseline airplane and the reference spanloader (fig. 2). The data developed in the course of the preceding analysis that are pertinent to the relation between these aircraft are summarized in figure 17. All the data presented correspond to a value of the nominal payload density D_{PL} of 136 kg/m^3 (8.5 lb/ft^3) – the value calculated for the reference spanloader. With this condition imposed, the configuration of the baseline airplane is preserved only at a reduced size and weight, and the resulting airplane is labeled "Baseline $\left(\text{adjusted } D_{PL}\right)$" in figure 17. The top part of the figure supplements the data presented in the lower parts and illustrates the change in airplane shape and size with increasing gross weight and for different values of W_G/S_W. No sketch is shown for the Boeing spanloader; however, as indicated by the symbols, its location on the figure is very close to the sketch given for the airplane scaled from the baseline to zero fuselage volume.

The curves of payload and block-fuel ratios for constant wing loading (solid lines) are compared with curves for constant $\overline{V}^{2/3}/S_W$, but with varying wing loading (dashed lines). It should be noted that for all plots in previous figures with $\overline{V}^{2/3}/S_W$ held constant, the wing loading also was constant while payload density varied. Appreciable displacements are noted between the solid curves for the high wing loading (baseline airplane) and those for the low wing loading (spanloader). No single path of any general significance can be shown for the transfer from one wing-loading level to the other, since many design and operating considerations are involved. For either the payload ratio or the block-fuel ratio, a somewhat more rapid improvement with increasing gross weight is shown when wing loading is constant (configuration tending toward all-wing) than when $\overline{V}^{2/3}/S_W$ is constant. In fact, for the idealized performance yardsticks presented, it would seem difficult to improve on the very large all-wing airplane (spanloader) with any wing-fuselage configuration. The indicated advantage of the spanloader over wing-fuselage

18

designs at approximately the same gross weight, however, is small; thus, it is possible that the advantages shown herein could be offset by other factors, such as may stem from design or economic considerations. It also should be borne in mind that essentially all the results presented in this paper apply only to a condition of bulk cargo capable of occupying available space in both fuselage and wing. This condition was necessary for the present study; however, the use of a fuselage exclusively to contain the payload is desirable in some applications of cargo aircraft. An interesting possibility might involve two or more separate fuselages so positioned along the span to derive some benefit in wing weight from distributed-load relief.

The trends shown in the present study might be altered considerably if methods under development for achieving laminar flow are proven to be practical for application to any of or all the airplane surfaces. If the application is made only to the wing, then any nonlaminarized surfaces should be minimized; this condition points to the spanloader as the course for achieving the greatest benefit. If, on the other hand, laminar flow is to be realized on the fuselage surface but not on the wing, then it may be desirable to provide relatively large single or multiple fuselages and minimize wing surface area by designing for the highest practical wing loading.

In a more general sense, it is noted that the benefit likely to be realized from a technology advance in any of the disciplines may depend strongly on many aspects of airplane design. The technique described has been found useful for identifying conditions under which such benefits may be most attractive. As presented herein, only basic airplane capabilities, as determined by physical disciplines, which do not include cost or economic factors, have been considered. The techniques described undoubtedly can be improved by additions to the data base and by refinements to the analytical process; these improvements should lead to improved versatility.

CONCLUDING REMARKS

A size-scaling procedure with empirical-data inputs has been used to explore the progression from current cargo aircraft of conventional wing-fuselage design to possible future cargo aircraft of all-wing (spanloader) design. Correlations of design data ranging from those available for current aircraft to those from advanced airplane studies by industry contractors were employed in conducting the analysis. The calculation method accounts for the change in relative size of wing and fuselage as airplane size is increased while the density of the payload remains constant, for corresponding changes in the ratio of tail area to wing area, and approximately for corresponding changes in bending-moment relief from span-distributed loading.

The study shows that when the nature of the payload is such that it can occupy the volume available in both fuselage and wing, a progressive increase in the ratio of payload

weight to airplane gross weight is realized as the airplane becomes larger and heavier. A reduction in the ratio of block-fuel weight to payload weight also is shown. When the fuselage is sized to accommodate all the payload, the payload—gross-weight ratio shows almost no variation up to gross weights of at least 17.79 MN (4×10^6 lb). These results indicate a more favorable outlook for the capabilities of very large aircraft than might be expected from first impressions of implications of the cube-square law. The results of this study however are consistent with the cube-square law, provided the law is applied separately to major airplane components rather than to the airplane as a unit.

The calculations show continued improvement in the payload and block-fuel ratios as the all-wing (or spanloader) condition is approached; however, for approximately the same gross weights, the improvement is small and is not necessarily the prevailing consideration in selection of the design of very large airplanes.

A check on the method was made by scaling from a current wing-fuselage design to the conditions that apply to a spanloader design that had been identified in an industry study. Close agreement of characteristics for the scaled airplane and the industry spanloader tends to support use of the technique as a tool for exploratory studies and for evaluating the benefits of advanced technologies.

Langley Research Center
National Aeronautics and Space Administration
Hampton, VA 23665
February 13, 1980

APPENDIX

AN EMPIRICAL EQUATION FOR ESTIMATING THE WING
WEIGHT OF SUBSONIC TRANSPORTS

To facilitate exploratory parametric analyses of future subsonic transport aircraft, a new empirical equation for estimating wing weight has been developed. Although limited by the data base to cruise Mach numbers from about 0.7 to 0.85, the equation provides a basis for exploring potential aircraft that are much larger than aircraft now in existence and of accounting for benefits of distributed loading and advanced structural technology. The new equation makes use of data from recent studies of a variety of advanced designs. The new data provide increased breadth of the data base and, therefore, improved accuracy in defining parametric trends. The equation still suffers from a lack of data for intermediate designs between conventional aircraft and spanloaders. It is believed, however, that the form of the equation is readily adaptable to future data additions which should improve the reliability of wing-weight estimations.

An intentional effort has been made to keep the equation relatively simple, since this is considered to be an advantage in exploratory analyses. In general, the level of detail is about equal to that of previous empirical wing-weight equations, such as are given in references 13 and 14 and of others that exist in unpublished industry documents. The sources which were available to the author were studied during the development of the equation described herein.

Basically, the new equation expresses wing weight as the sum of the weights of two subgroups. One approximates the material weight required to resist spanwise bending and the other approximates the sum of material weights required to resist all other loads. In comparing the weights for conventional and spanloader designs, it will be noted that whereas the miscellaneous term may have almost the same value for either class, the bending term may predominate for conventional designs but be relatively insignificant for spanloaders.

The proposed equation for wing weight per unit wing area is

$$\frac{W_W}{S_W} = K_{ST}\left(C_1 K_{LD}\frac{I_B}{S_W} + C_2\frac{I_M}{S_W}\right) \tag{A1}$$

where

K_{ST} structural technology factor, varies from 1.0 for current aluminum structures to about 0.75 for advanced structures with 50 percent to 60 percent composites

K_{LD} load distribution relief factor with a value of about 0.8 for current transports having four engines on the wing and about 0.3 for advanced spanloaders

$$\frac{I_B}{S_W} = \frac{U}{t/c}\left(\frac{W_{ZF}}{W_G}\right)^{0.5}\left(\frac{1+2\lambda}{1+\lambda}\right)\left(\frac{A^{3/2}}{\cos^2 \Lambda_{c/4}} + 6\right)\left(\frac{W_G}{S_W}\right)^{0.7} S_W^{0.5} \times 10^{-6}$$

$$\frac{I_M}{S_W} = \left(1 + \frac{t}{c}\right)\left[1 + C_3\left(\frac{W_G}{S_W}\right)^{0.1}\right] S_W^{0.05}$$

and C_1, C_2, and C_3 are correlation constants, whose values for the two systems of units are as follows:

	SI	U.S. Customary
C_1	43.4	4.14
C_2	85.7	1.59
C_3	0.68	1

A previous correlation of wing-weight data from current conventional transports and from industry studies of advanced technology spanloaders had been made for use in analyses involving airplane size scaling, in which the wing shape remains constant while the size of the wing varies. Results of this correlation are summarized in figure A1. The aircraft considered in developing the correlation for the conventional class were restricted to jet-powered swept-wing transports designed to meet commercial specifications. Variations of the nondimensional wing geometry parameters A, λ, $\Lambda_{c/4}$, and t/c were moderate for the conventional group and somewhat larger for the spanloaders; nevertheless, for use in size scaling with constant shape, an acceptable approximation for either class of aircraft is obtained with a correlation expression of the form:

$$W_W \propto S_W^{n'}$$

or

$$\frac{W_W}{S_W} \propto S_W^{(n'-1)}$$

APPENDIX

The approximation, when expressed in terms of the linear scale ratio L with the alternate scaling exponent n, becomes

$$W_W \propto L^n$$

where

$$n = 2n'$$

To express a best fit with a given set of data, the proportionality sign must be replaced by a correlation coefficient K. Therefore, an equation in the form used to define the summary curves of figure A1 is

$$\frac{W_W}{S_W} = KS_W^{(n'-1)} \tag{A2}$$

where values of K and the exponent (n'-1) appear in the relations given for the curves representing each of the various conditions summarized. It should be noted that the coefficient K, although essential in developing empirical relations, is of no significance in problems involving scaling from a defined baseline.

The curve labeled "Current technology" for the conventional class was obtained from the correlation of data for current transports. Results from the studies of references 9 to 11 suggested that the technology available in the 1995 to 2000 time period should permit a wing weight reduction of about 25 percent. The data available from industry studies of spanloaders (refs. 1 to 4) already included technology advances expected to be available in the 1995 to 2000 time period and therefore provided the basis for an "Advanced technology" curve for spanloaders. The curve for "Current technology," in this case, was obtained by increasing the level of the "Advanced technology" curve by 25 percent. It should be noted that a 25-percent weight reduction from current technology is represented in the general wing-weight equation by a value of the structural technology factor K_{ST} equal to 0.75.

Figure A2 compares values of wing weight when calculated by the general equation with the actual airplane wing weight used in the conventional aircraft correlation. Calculated curves are shown for wing loadings of 4788 and 6703 N/m^2 (100 and 140 lb/ft^2), while average values of A, t/c, λ, and $\Lambda_{c/4}$ were prescribed and held constant over the range of wing reference areas for the aircraft considered. The calculated curves provide a good representation of the trend of the airplane data, and many — although not all — data points fall between the curves for the two wing loadings. Also, the curves

23

calculated from the general equation are generally consistent with the simple scaling relation $W_W = KS_W^{1.35}$.

A similar comparison for spanloaders is given in figure A3. In this case, the general equation was used to calculate curves for wing loadings of 3352 and 4788 N/m^2 (70 and 100 lb/ft^2), and other wing parameters were held constant at the approximate averages of the data available. The general equation provides reasonable agreement with the data and with the simple scaling relation $W_W = KS_W^{1.1}$.

In the present state of the wing-weights data base, judgment must be exercised in evaluating the load-distribution relief factor K_{LD}. This factor represents the ratio of bending-material weight for an arbitrary configuration to bending-material weight for an airplane having no relief from spanwise distribution of items such as engines, fuel, payload, and landing gear. For the present development, as a starting point, current transports with four engines on the wing were assumed to have 20-percent bending-load relief; that is, $K_{LD} = 0.8$. A value for spanloaders, $K_{LD} = 0.3$, then was obtained from the correlation process after differences in wing geometry and structural technology had been accounted for. These two values can be used to provide a crude basis of estimating K_{LD} for arbitrary aircraft by using figure A4. As figure A4 indicates, consideration has to be given to load relief in flight and to load relief on the ground in order to determine a value of K_{LD} (the design factor). At present, the relative importance of flight and ground relief is not established; however, for the purpose of constructing figure A4, it was assumed that ground relief contributes half as much to K_{LD} as does flight relief. It can be inferred from figure A4 that although fairly reliable values of K_{LD} can be estimated for conventional designs and for spanloaders, considerable uncertainty is associated with estimates for designs that are intermediate to these two classes, because of a shortage of applicable data.

REFERENCES

1. Whitlow, David H.; and Whitener, P. C.: Technical and Economic Assessment of Span-Distributed Loading Cargo Aircraft Concepts. NASA CR-144963, 1976.

2. Technical and Economic Assessment of Span-Loaded Cargo Aircraft Concepts. NASA CR-144962, 1976.

3. Johnston, William M.; Muehlbauer, John C.; Eudaily, Roy R.; Farmer, Ben J.; Honrath, John F.; and Thompson, Sterling G.: Technical and Economic Assessment of Span-Distributed Loading Cargo Aircraft Concepts. NASA CR-145034, 1976.

4. Preliminary Design Dep., Boeing Commercial Airplane Co.: Technical and Economic Assessment of Swept-Wing Span-Distributed Load Concepts for Civil and Military Air Cargo Transports. NASA CR-145229, 1977.

5. Whitener, P. C.: Distributed Load Aircraft Concepts. J. Aircr., vol. 16, no. 2, Feb. 1979, pp. 72-77.

6. Cleveland, F. A.: Size Effects in Conventional Aircraft Design. J. Aircraft, vol. 7, no. 6, Nov.-Dec. 1970, pp. 483-512.

7. Keith-Lucas, David: Defeating the Square-Cube Law. Flight Int., vol. 94, no. 3106, Sept. 19, 1968, pp. 440-442.

8. Laser: Design Probe. Another Look at the Square Cube Law. Flight Int., vol. 94, no. 3110, Oct. 17, 1968, pp. 615-616.

9. Study of the Application of Advanced Technologies to Long-Range Transport Aircraft. Volume II – Technology Applications. Contract No. NAS 1-10702, Convair Aerospace Div., General Dynamics, Aug. 5, 1972. (Available as NASA CR-112090.)

10. Lange, R. H.; Sturgeon, R. F.; Adams, W. E.; Bradley, E. S.; Cahill, J. F.; Eudaily, R. R.; Hancock, J. P; and Moore, J. W.: Study of the Application of Advanced Technologies to Long-Range Transport Aircraft. Volume I – Analysis and Design. Contract No. NAS 1-10701, Lockheed-Georgia Co., Lockheed Aircraft Corp., [1972]. (Available as NASA CR-112088.)

11. Final Report – Study of the Application of Advanced Technologies to Long-Range Transport Aircraft. Volume I – Advanced Transport Technology Final Results. Contract No. NAS 1-10703, Boeing Co., May 1972. (Available as NASA CR-112092.)

12. Jernell, Lloyd S.: Preliminary Study of a Large Span-Distributed-Load Flying-Wing Cargo Airplane Concept. NASA TP-1158, 1978.

13. Oman, B. H.: Vehicle Design Evaluation Program. NASA CR-145070, 1977.

14. Beltramo, Michael N.; Trapp, Donald L.; Kimoto, Bruce W.; and Marsh, Daniel P.: Parametric Study of Transport Aircraft Systems Cost and Weight. NASA CR-151970, 1977.

TABLE I.- APPLICATION OF ADVANCED TECHNOLOGY FACTORS FOR DERIVING

BASELINE AIRPLANE FROM BOEING 747-200F

Item	Boeing 747-200F (relative value)	Baseline		
		Relative value	Actual value	
			N	lb
Weights:				
Wing	W_W	$0.8W_W$	313 900	70 600
Tail	W_T	$0.8W_T$	65 600	14 700
Body	W_B	$0.8W_B$	359 800	80 900
Landing gear.	W_L	$0.9W_L$	129 300	29 100
Propulsion	W_P	$0.95W_P$	239 400	53 800
Equipment	W_E	$1.0W_E$	177 900	40 000
Specific fuel consumption . . .	SFC	0.9SFC	------	-----
Design range, km (n. mi.) . .	5334 (2880)	5556 (3000)	------	-----
Wing airfoil	Boeing	Supercritical	------	-----
Wing thickness	t/c varies	t/c = 0.13	------	-----

27

TABLE II.- VALUES OF SCALING EXPONENTS AND TYPICAL WEIGHT FRACTIONS

FOR PRIMARY TRANSPORT-AIRPLANE COMPONENTS
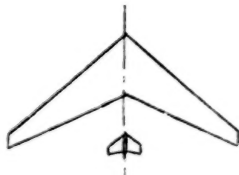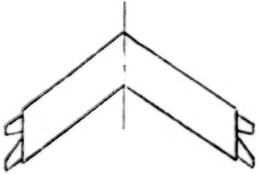
Component	Scaling exponent symbol	Value of scaling exponent		Typical fraction of gross weight (advanced technology aircraft)	
		Simple Cube/Square	Semi-empirical	Conventional	Spanloader
Wing	n_W	3	[a]2.7 [b]2.2	0.11	0.11
Tail	n_T	3	2.7	.025	.015
Body	n_B	3	2.5	.10	0
Landing gear	n_L	2	2	.05	.05
Propulsion[c]	n_P	---	2	.065	.065
Equipment and crew	n_E	---	2	.05	.05
Operating weight				.40	.29

[a]Conventional design.

[b]Spanloader design.

[c]Includes engines, nacelles, pylons.

TABLE III.- COMPARISON OF VARIOUS SIGNIFICANT QUANTITIES FOR BOEING 759-211 SPANLOADER AND AIRCRAFT DERIVED BY EXTRAPOLATION FROM BASELINE

Quantity	Baseline extrapolation	Adjusted baseline extrapolation	Boeing 759-211
L/D	24.4	21.7	21.7
W_G, N (lbf)	12 894 700 (2 898 900)	12 894 900 (2 898 900)	12 582 200 (2 828 600)
W_S, N (lbf)	2 633 800 (592 100)	2 330 400 (523 900)	2 217 900 (498 600)
W_W and W_T, N (lbf) . . .	2 152 100 (483 800)	1 848 700 (415 600)	1 662 700 (373 800)
W_L, N (lbf)	481 700 (108 300)	481 700 (108 300)	555 200 (124 800)
W_P, N (lbf)	891 900 (200 500)	891 900 (200 500)	890 500 (200 200)
W_E, N (lbf)	663 200 (149 100)	663 200 (149 100)	593 400 (133 400)
W_F, N (lbf)	2 256 100 (507 200)	2 250 800 (506 000)	2 261 400 (508 400)
$W_{F,B}$, N (lbf)	1 757 500 (395 100)	1 979 900 (445 100)	1 989 200 (447 200)
$W_{F,R}$, N (lbf)	498 600 (112 100)	270 900 (60 900)	272 200 (61 200)
W_{PL}, N (lbf)	6 449 700 (1 450 000)	6 758 600 (1 519 400)	6 619 000 (1 488 000)
W_{PL}/W_G	0.500	0.524	0.526
$W_{F,B}/W_{PL}$	0.273	0.293	0.301

29
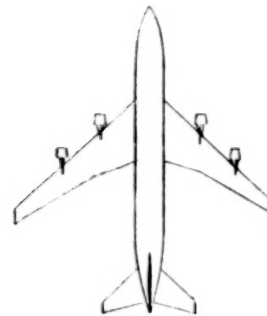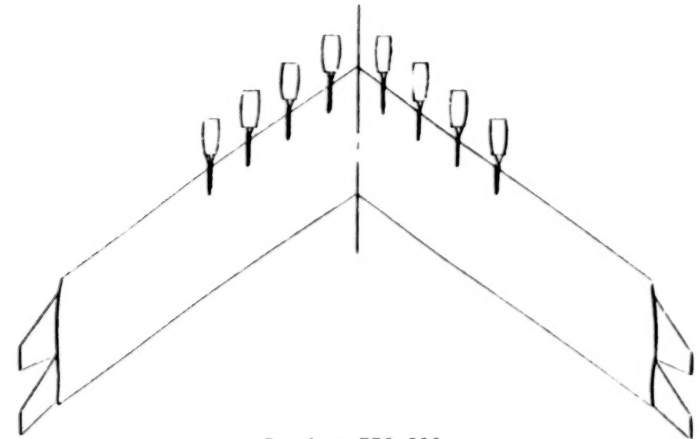
	Baseline		Boeing 759-211	
Gross weight, N (lbf)	3 460 700	(778 000)	12 582 200	(2 828 600)
Wing area, m² (ft²)	510.97	(5 500)	3 784.03	(40 731)
Wing loading, N/m² (lbf/ft²)	6 751	(141)	3 325	(69.45)
Wing span, m (ft)	59.65	(195.7)	136.2	(447)
Geometric aspect ratio	6.96		4.91	
Taper ratio	0.25		1.00	
Sweepback, deg	37.5		35	
Wing thickness ratio	0.13		0.131	
Specific fuel consumption, kg/N hr (lbm/lbf hr) ..	0.0571	(0.56)	0.0571	(0.56)
Range, km (n. mi.)	5 556	(3 000)	5 556	(3 000)
Cruise Mach number	0.85		0.85	
Payload, N (lbf)	1 329 600	(298 900)	6 619 000	(1 488 000)
Block fuel, N (lbf)	658 300	(148 000)	1 989 200	(447 200)
Reserve fuel, N (lbf)	186 800	(42 000)	272 200	(61 200)

Figure 1.- Reference airplanes.
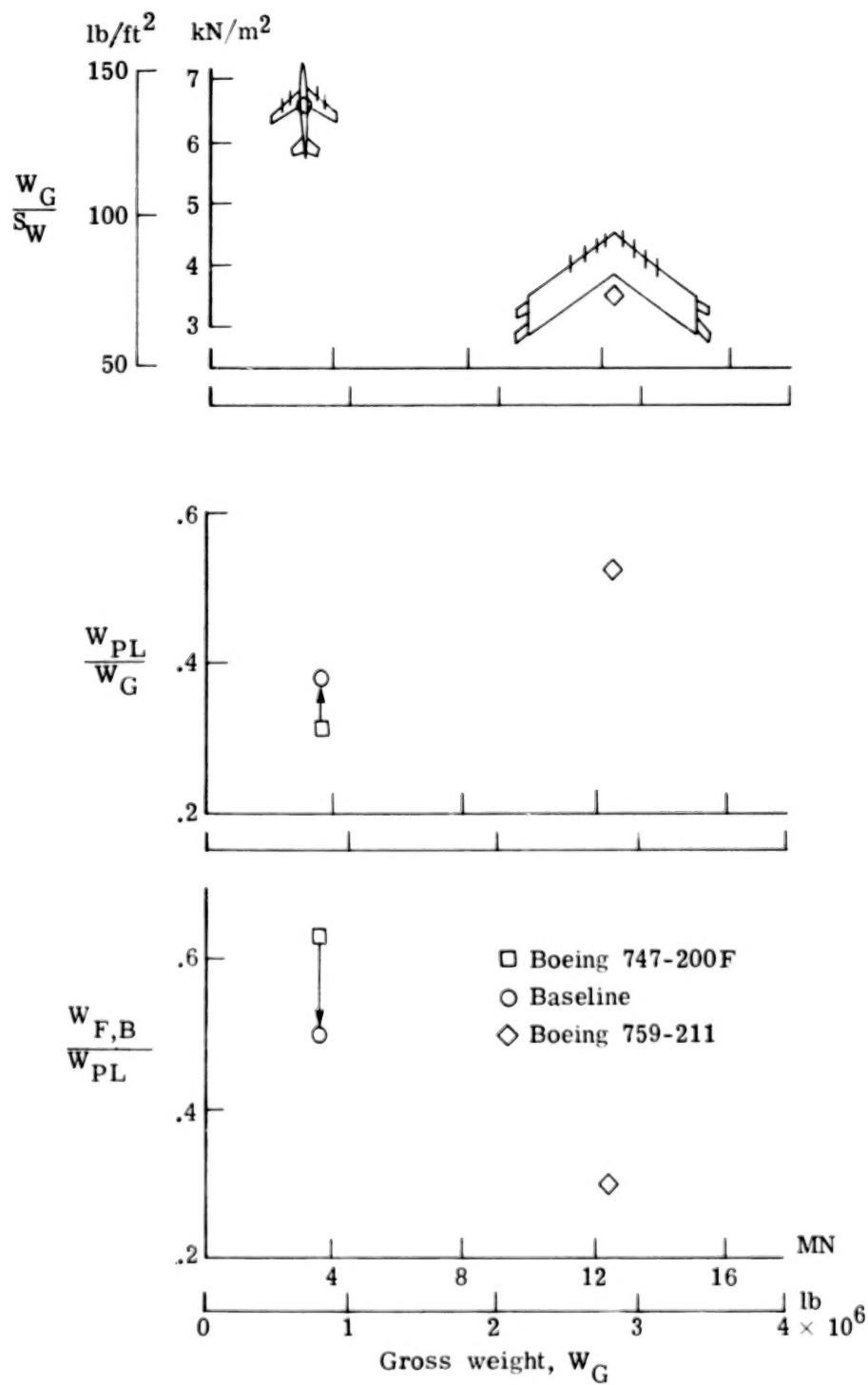
Figure 2.- Wing loading, payload ratio, and block-fuel ratio for reference airplanes.
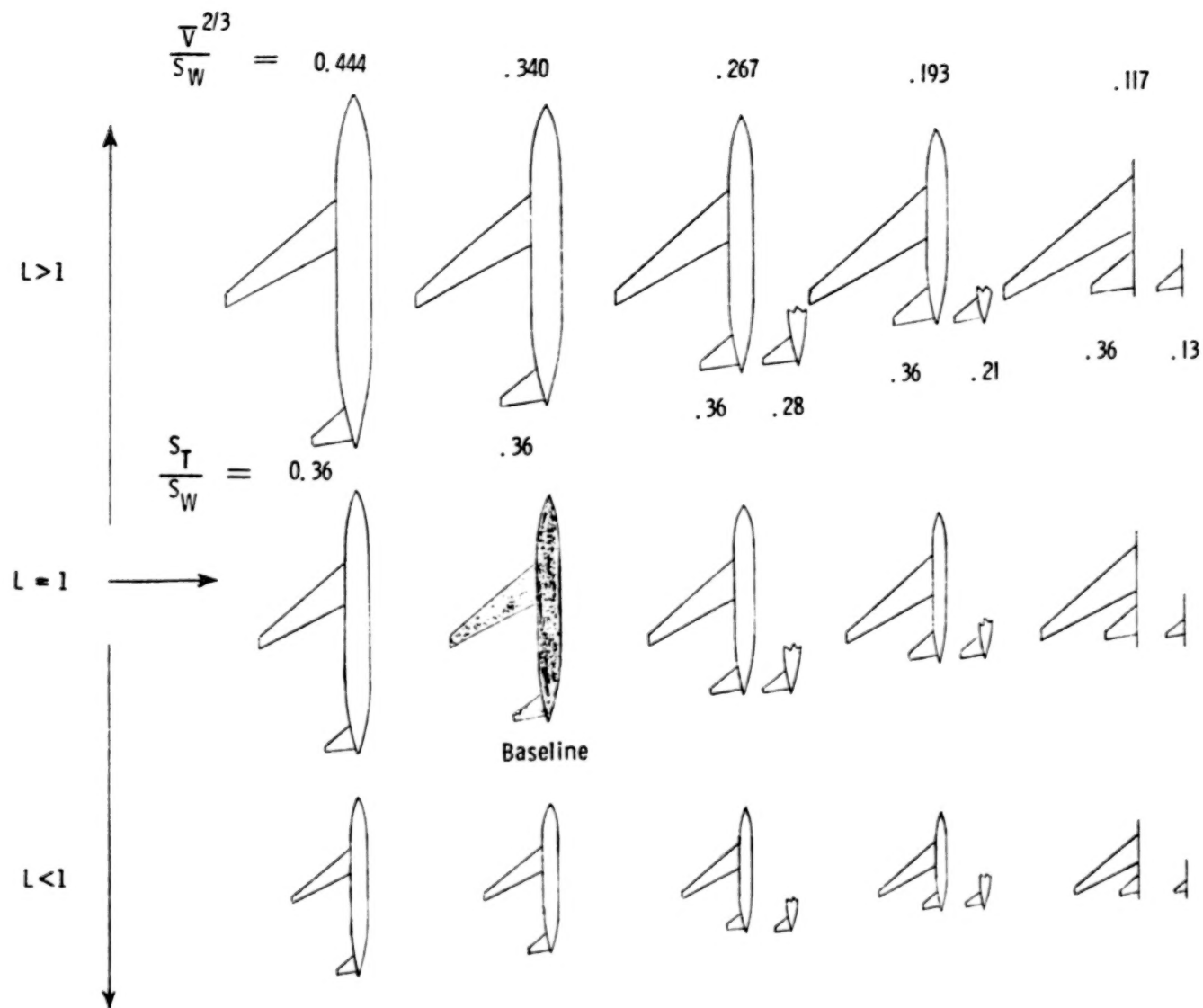
Figure 3.- Aircraft size and shape matrix defined for calculations.
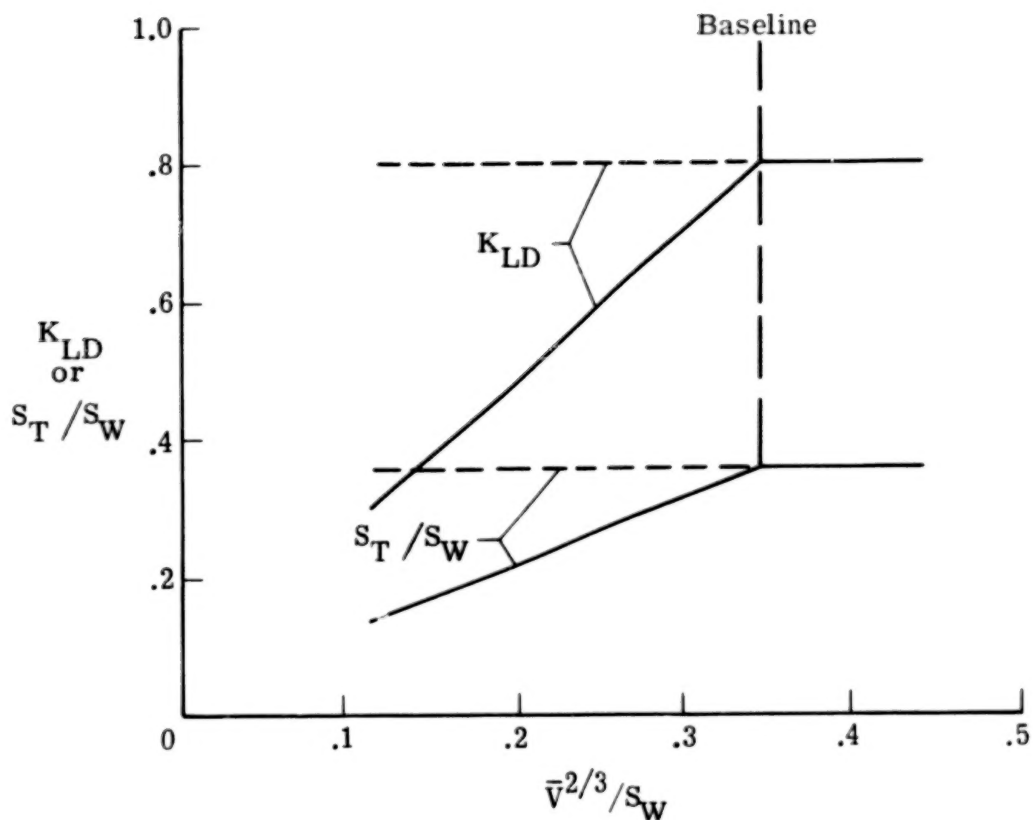
(a) Alternate variations of load-distribution relief factor
and of tail-area ratio with $\overline{V}^{2/3}/S_W$.
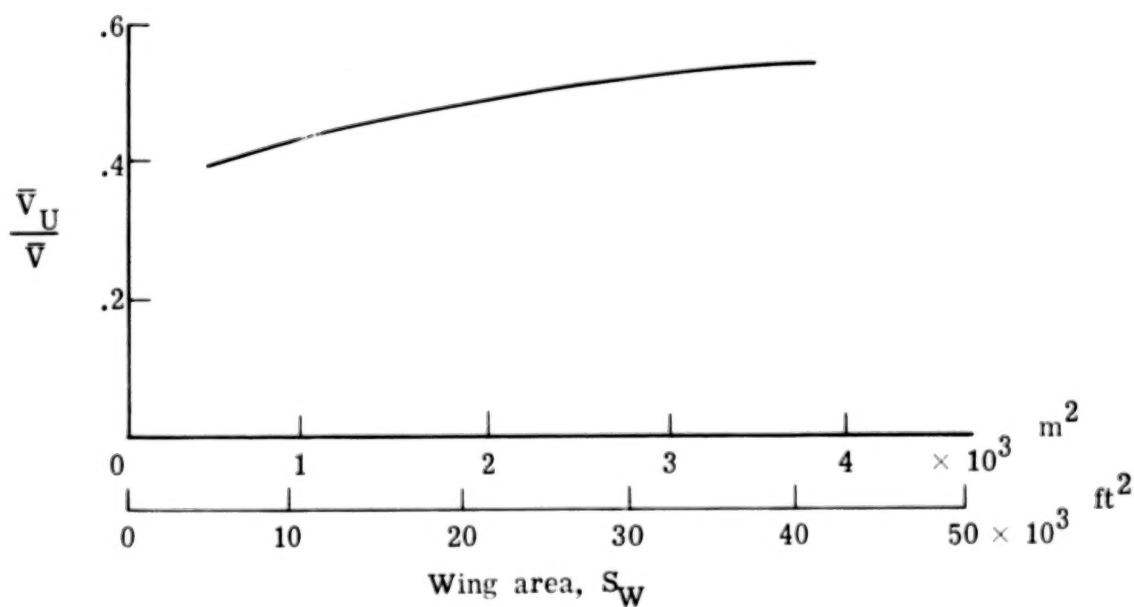
(b) Variation of wing-usable-volume ratio with wing area.

Figure 4.- Assumed values of parameters used in calculations.
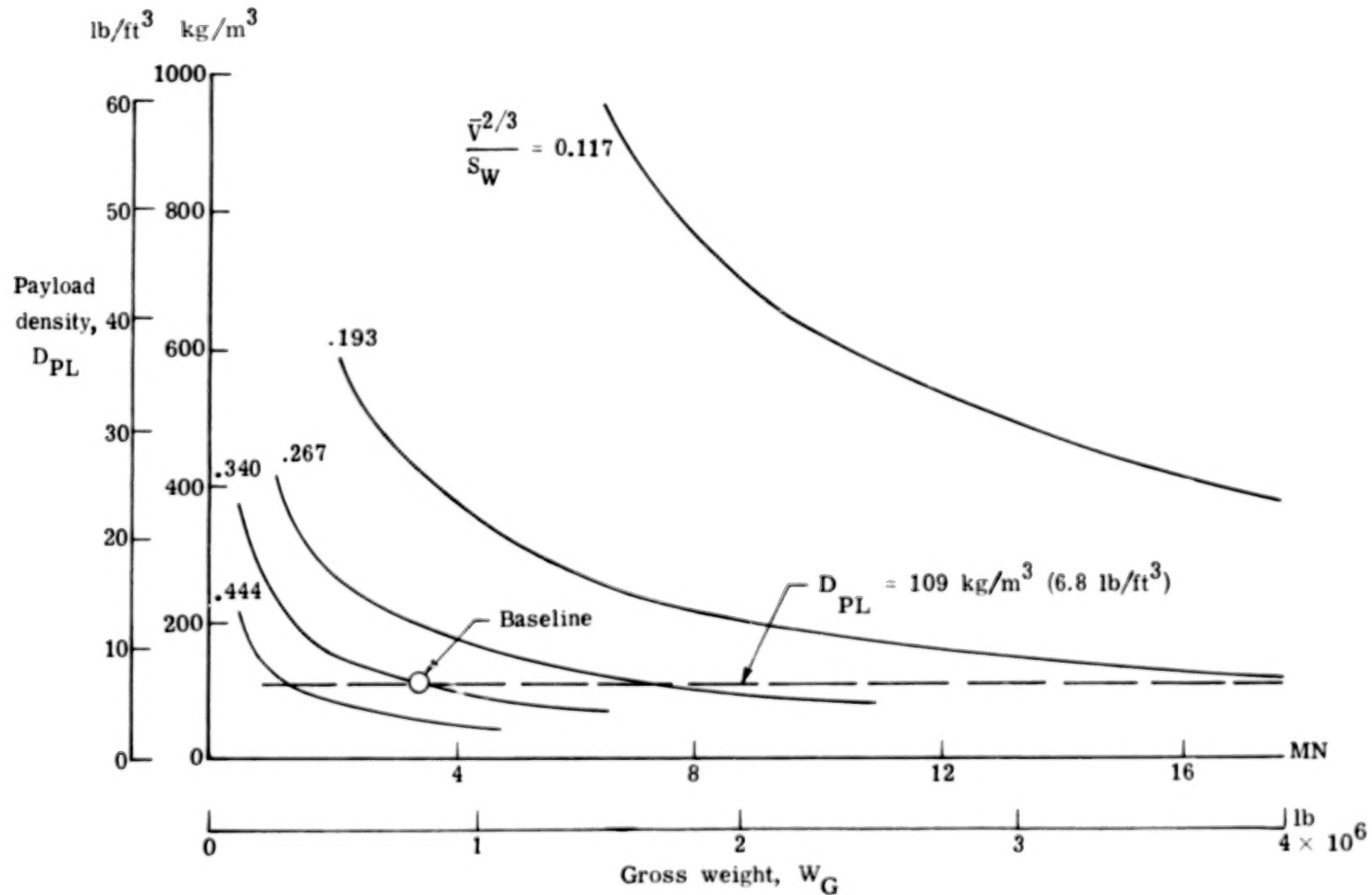
Figure 5. - Payload-density characteristics. $W_G/S_W = 6751$ N/m^2 (141 lb/ft^2); payload in body and wing; K_{LD} varies; S_T/S_W varies; scaling laws from semiempirical column of table II but with wing weight defined by general equation of appendix.
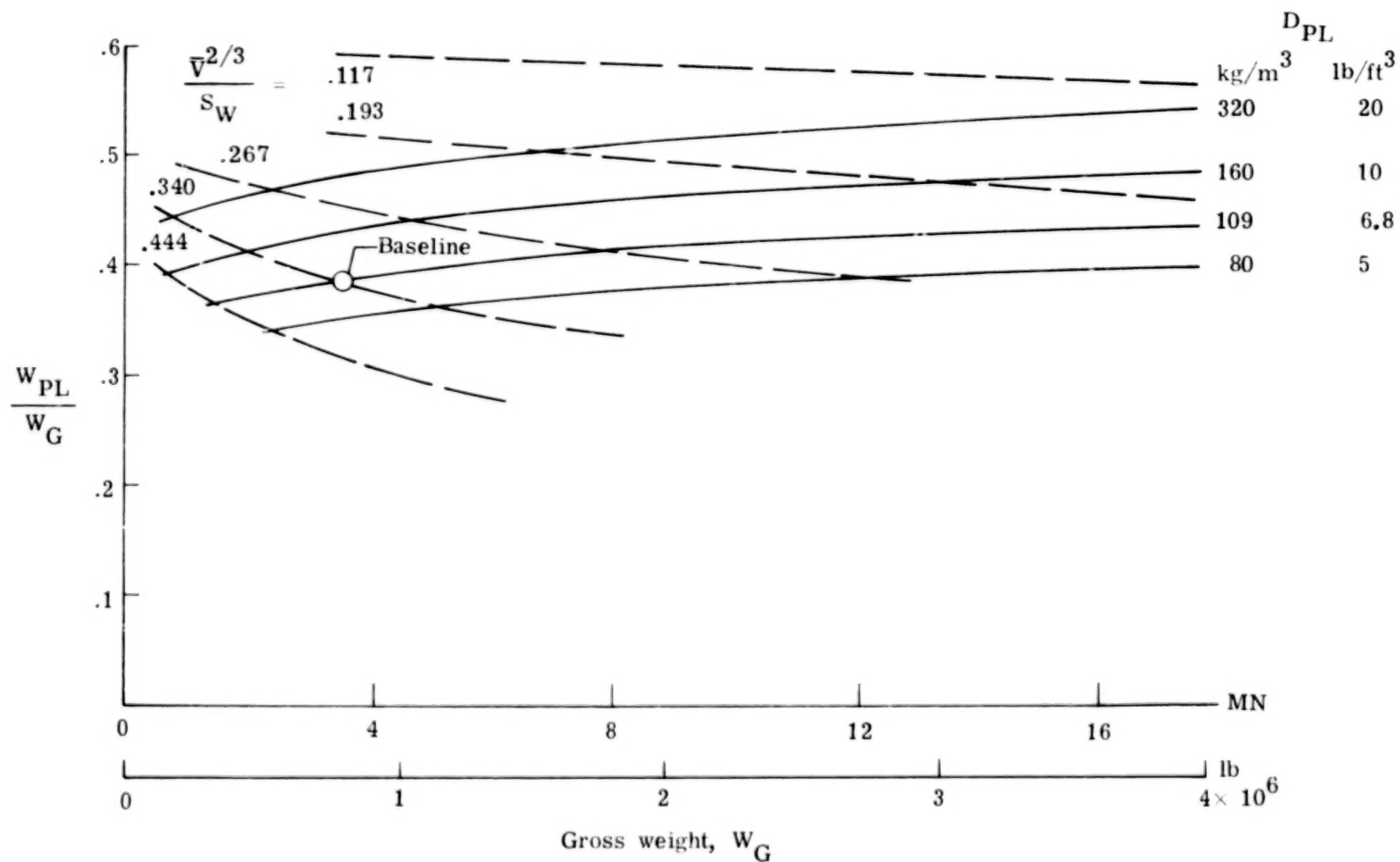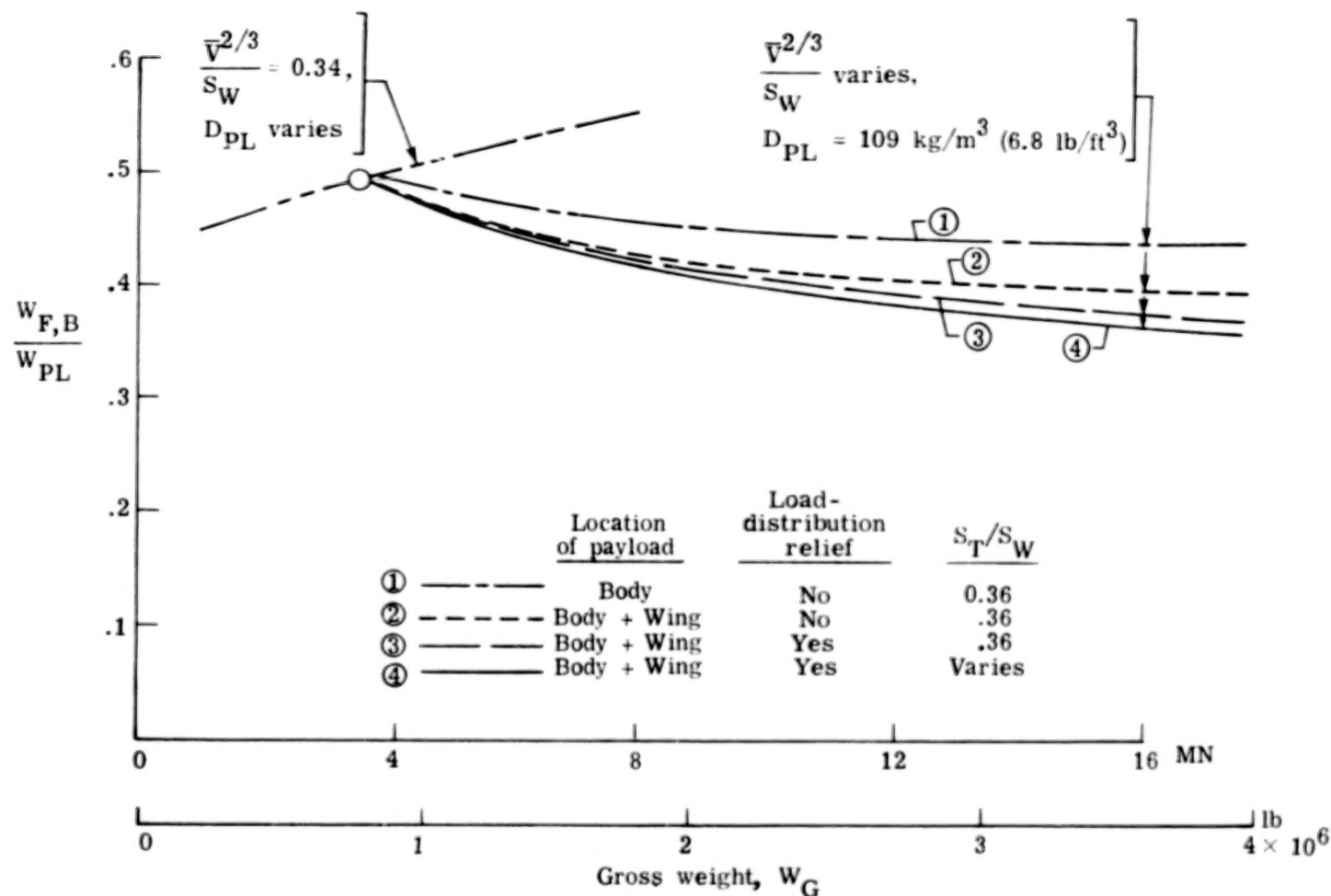
Figure 6.- Payload-ratio characteristics. W_G/S_W = 6751 N/m^2 (141 lb/ft^2); payload in body and wing; K_{LD} varies; S_T/S_W varies; scaling laws from semiempirical column of table II but with wing weight defined by general equation of appendix.
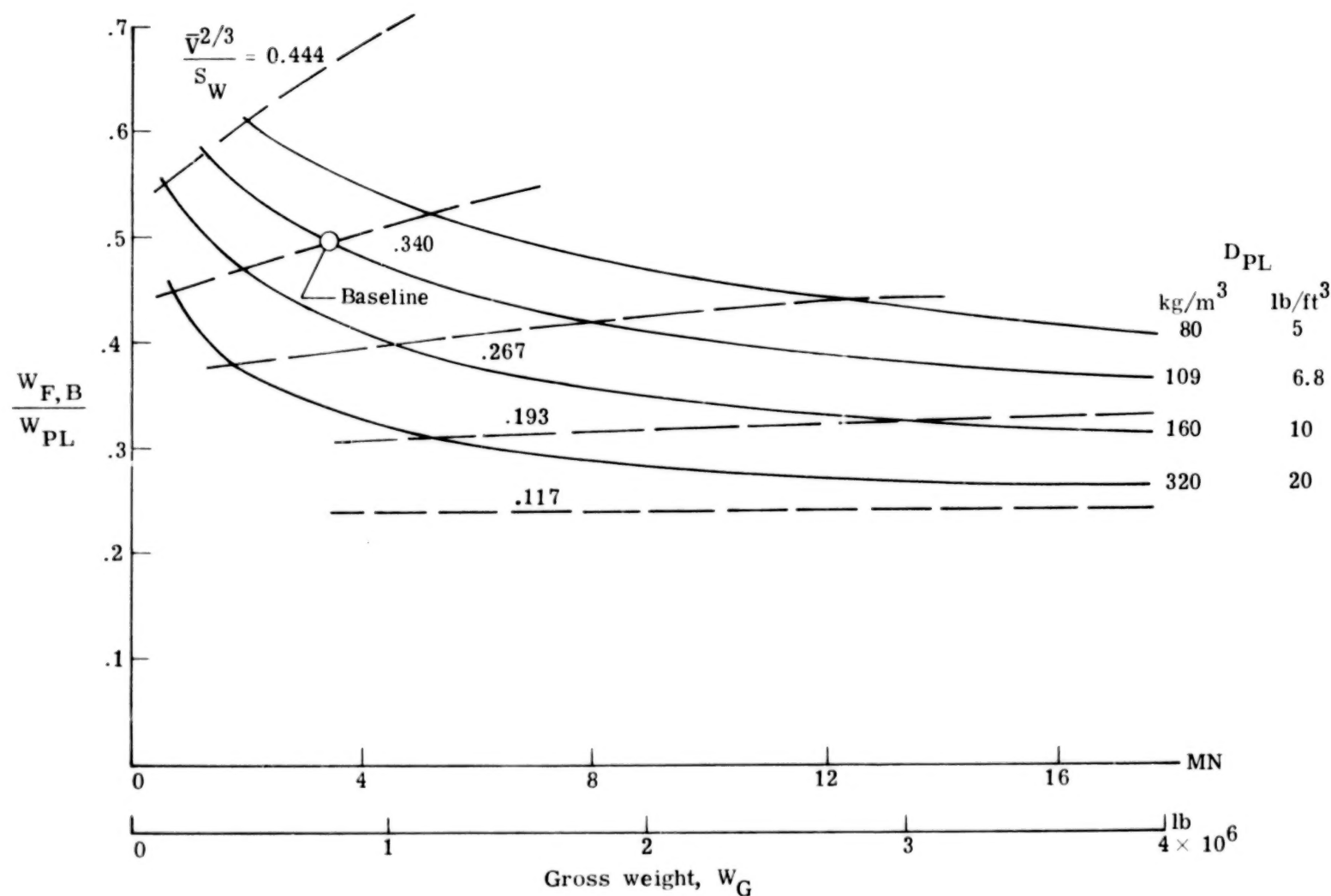
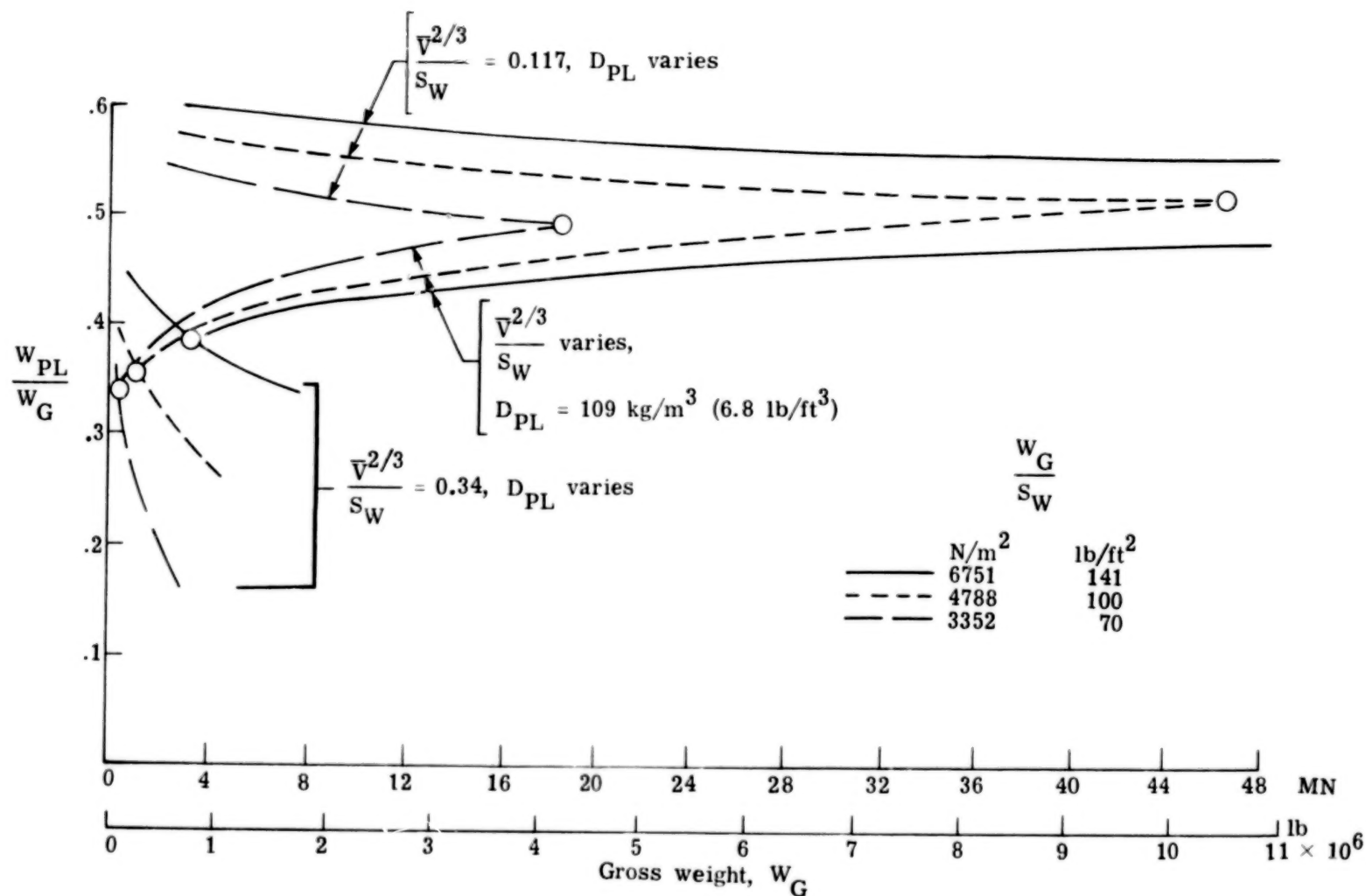Figure 7.- Block-fuel-ratio characteristics. $W_G/S_W = 6751$ N/m^2 (141 lb/ft^2); payload in body and wing; K_{LD} varies; S_T/S_W varies; scaling laws from semiempirical column of table II but with wing weight defined by general equation of appendix.
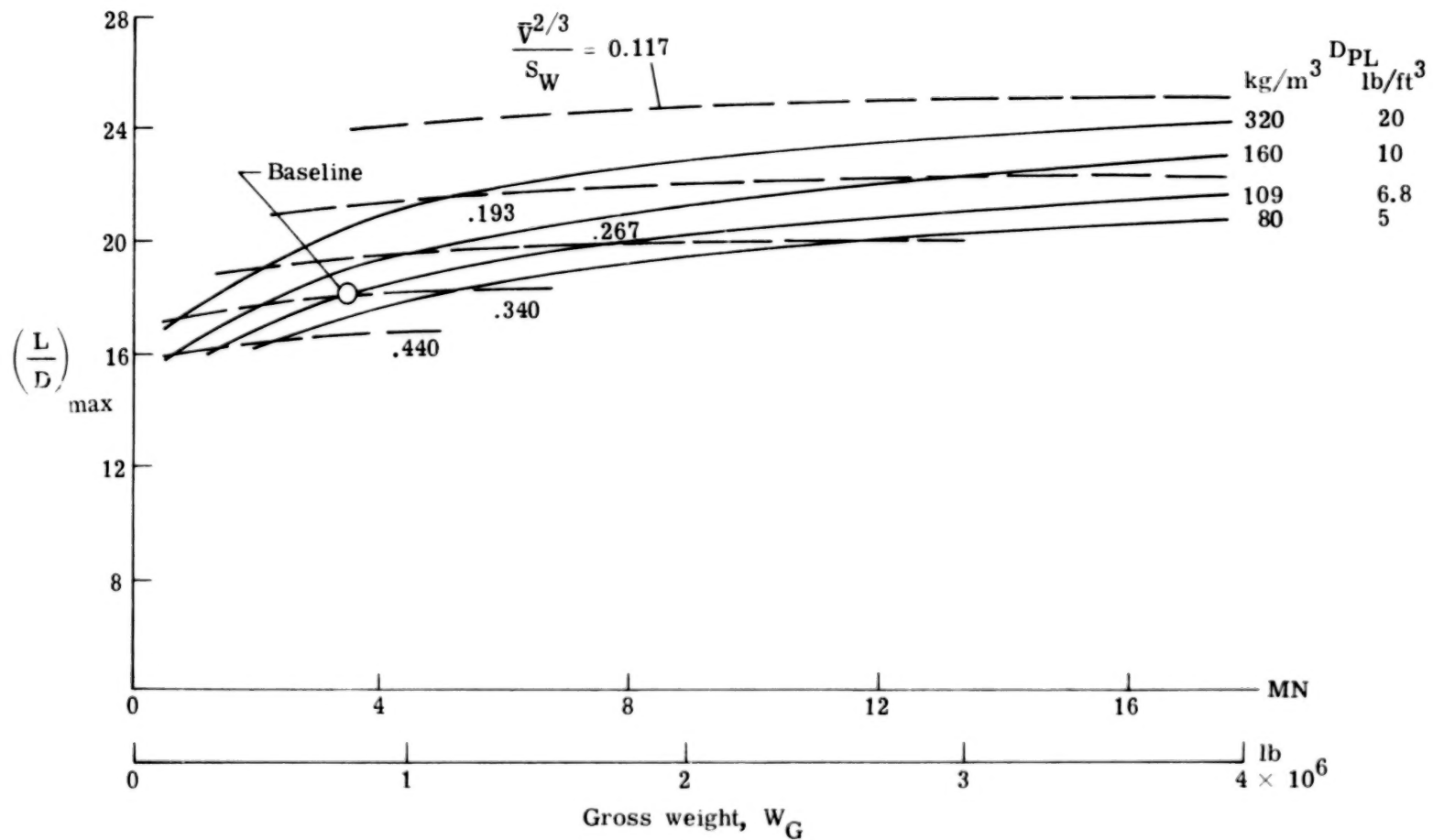
Figure 8.- Maximum L/D characteristics. $W_G/S_W = 6751$ N/m^2 (141 lb/ft^2); payload in body and wing; K_{LD} varies; S_T/S_W varies; scaling laws from semiempirical column of table II but with wing weight defined by general equation of appendix.
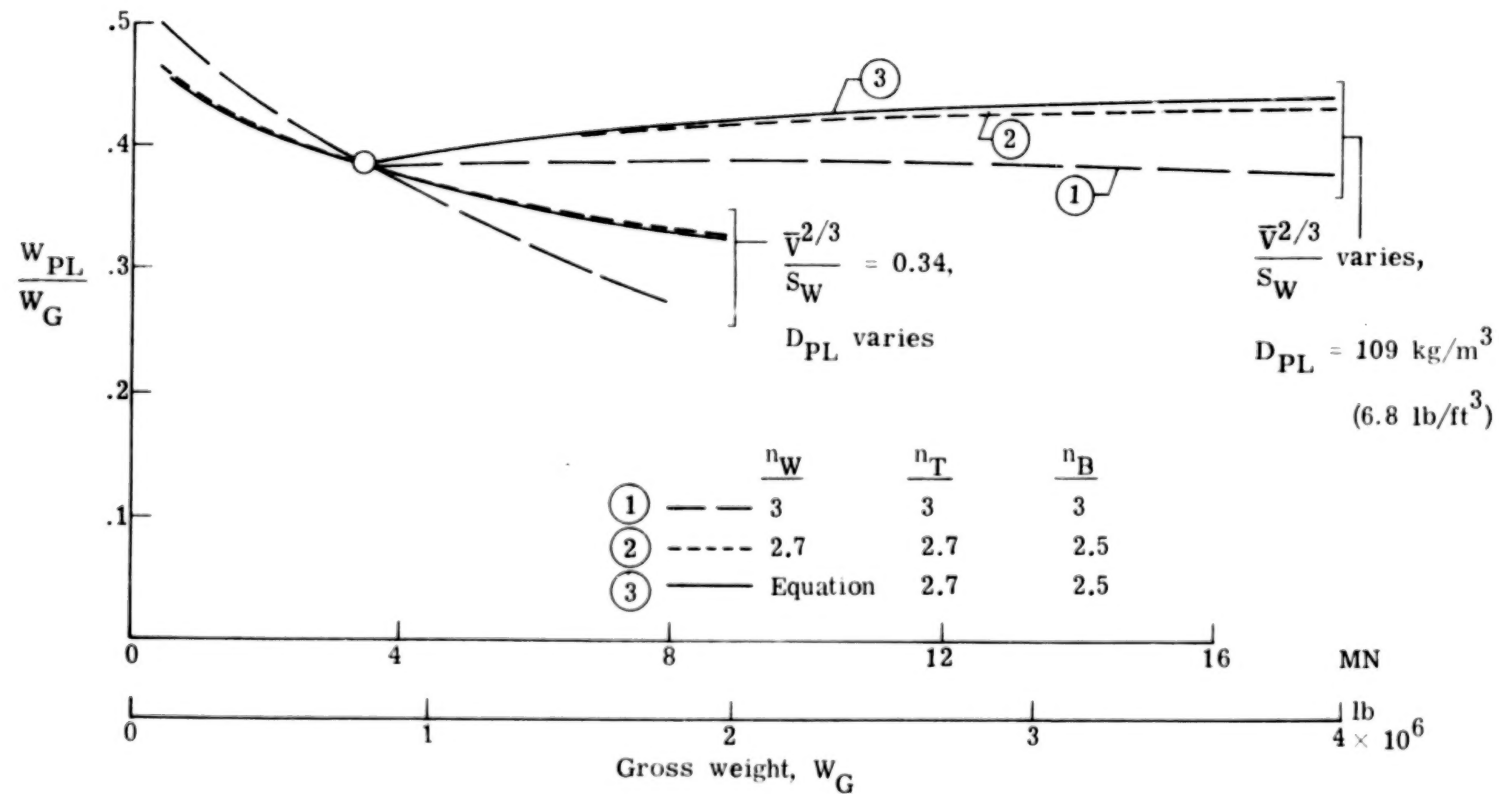
Figure 9.- Sensitivity of payload ratio to weight-scaling laws. $W_G/S_W = 6751$ N/m^2 (141 lb/ft^2); payload in body and wing; K_{LD} varies; S_T/S_W varies.
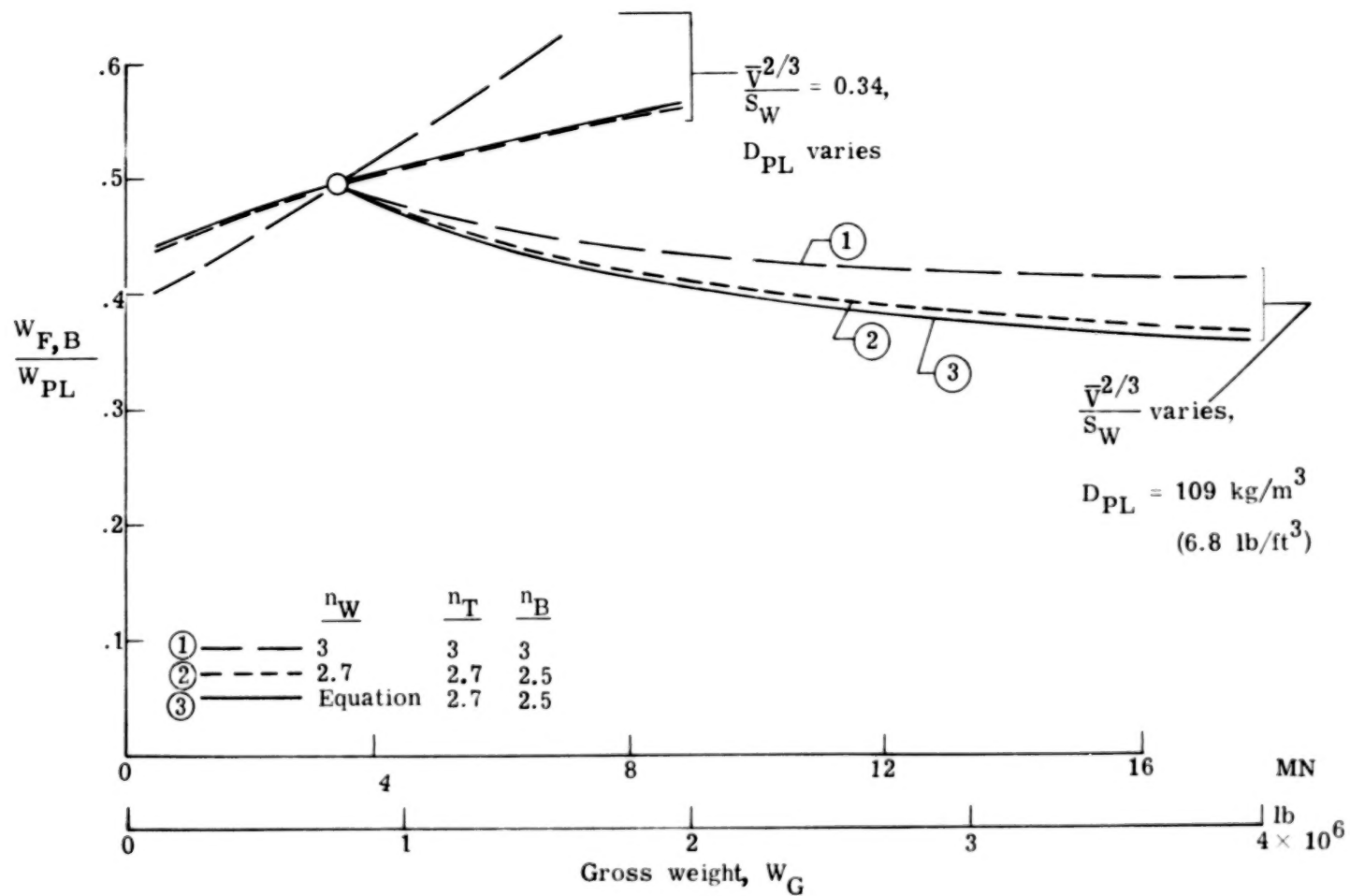
Figure 10.- Sensitivity of block-fuel ratio to weight-scaling laws. W_G/S_W = 6751 N/m² (141 lb/ft²); payload in body and wing; K_{LD} varies; S_T/S_W varies.

39
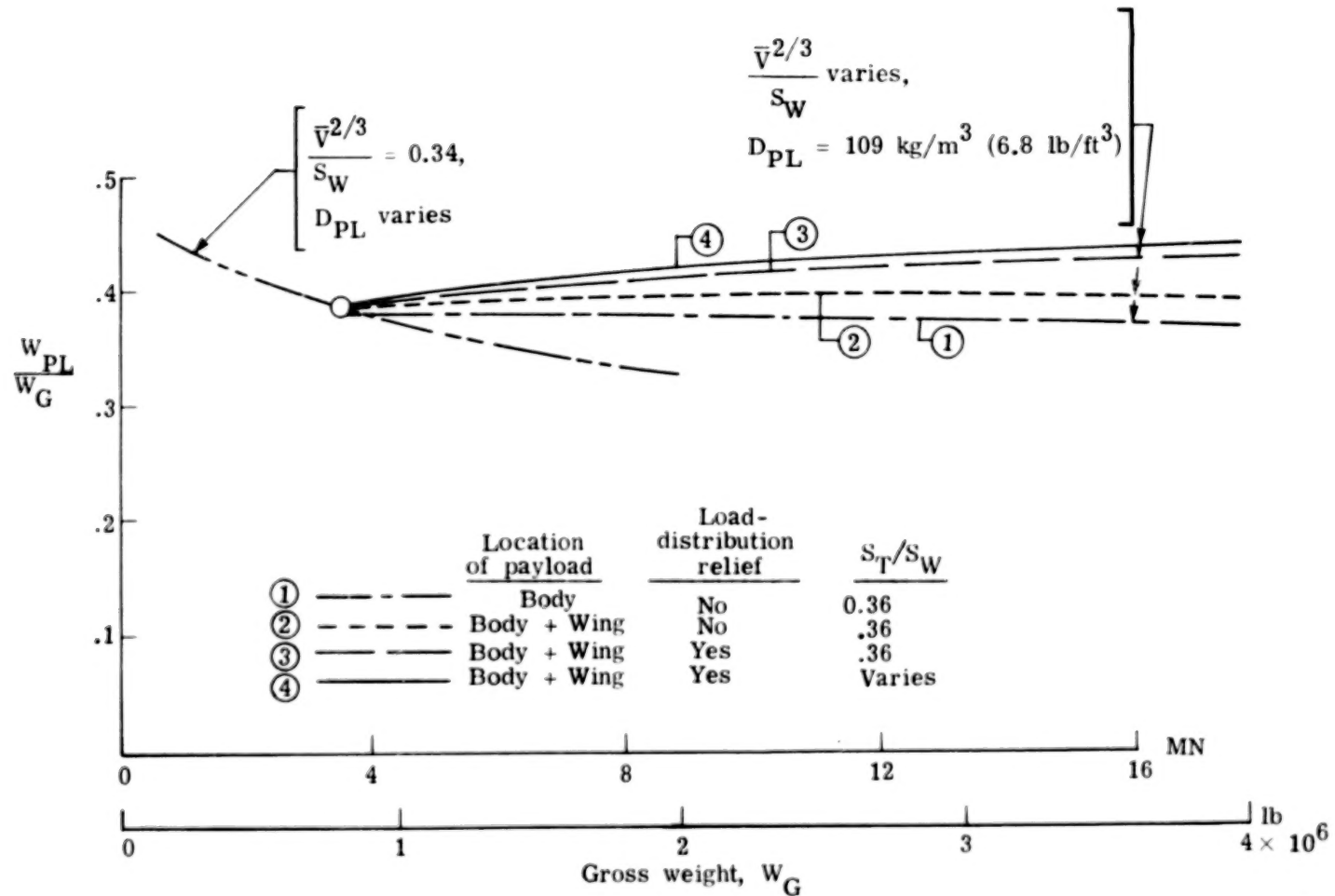
Figure 11.- Sensitivity of payload ratio to various assumptions. $W_G/S_W = 6751$ N/m^2 (141 lb/ft^2); scaling laws from semiempirical column of table II but with wing weight defined by general equation of appendix.

Figure 12.- Sensitivity of block-fuel ratio to various assumptions. $W_G/S_W = 6751 \text{ N/m}^2$ (141 lb/ft^2); scaling laws from semiempirical column of table II but with wing weight defined by general equation of appendix.

Figure 13.- Effect of wing loading and gross weight on payload ratio. Payload in body and wing; K_{LD} varies; S_T/S_W varies; scaling laws from semiempirical column of table II but with wing weight defined by general equation of appendix.
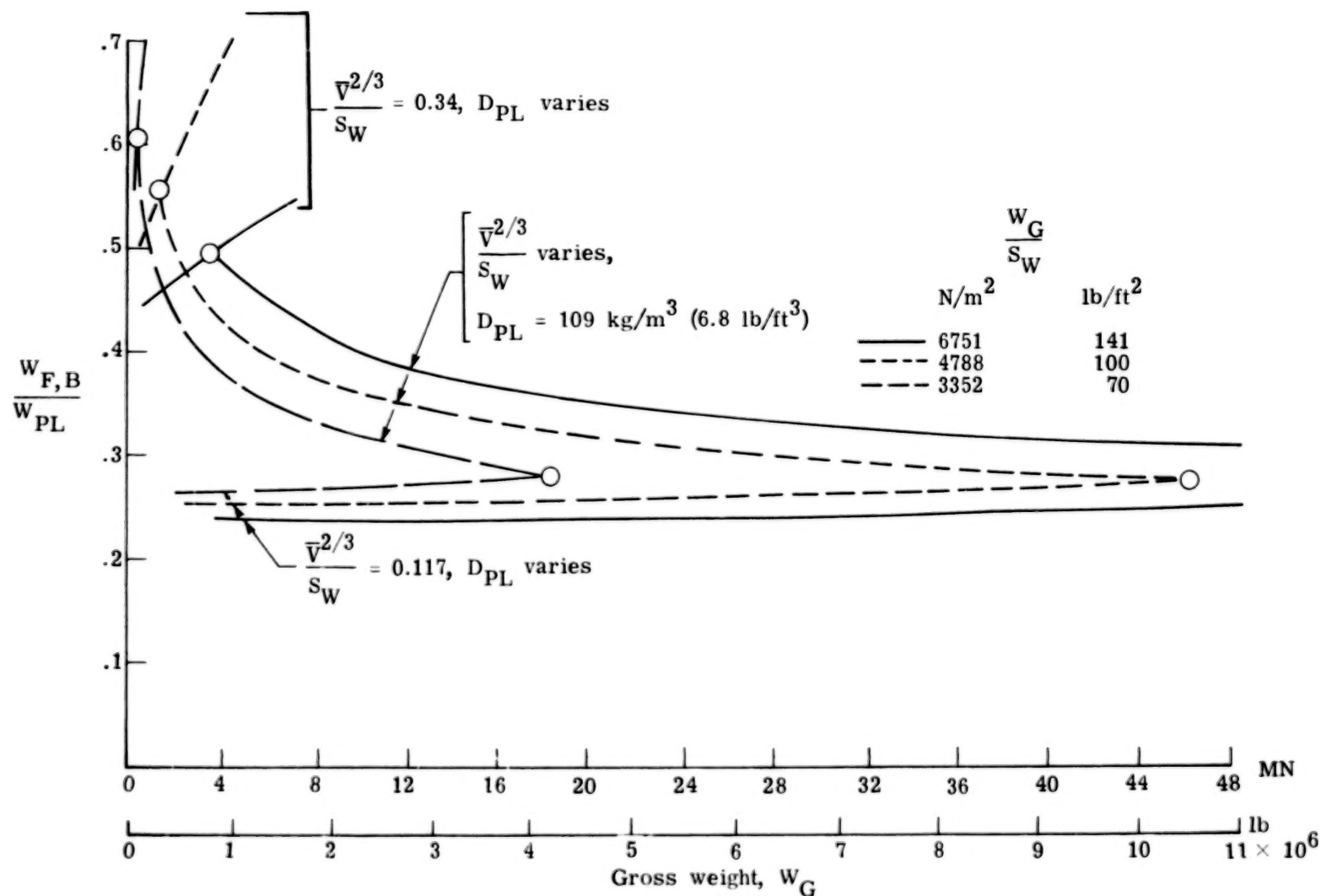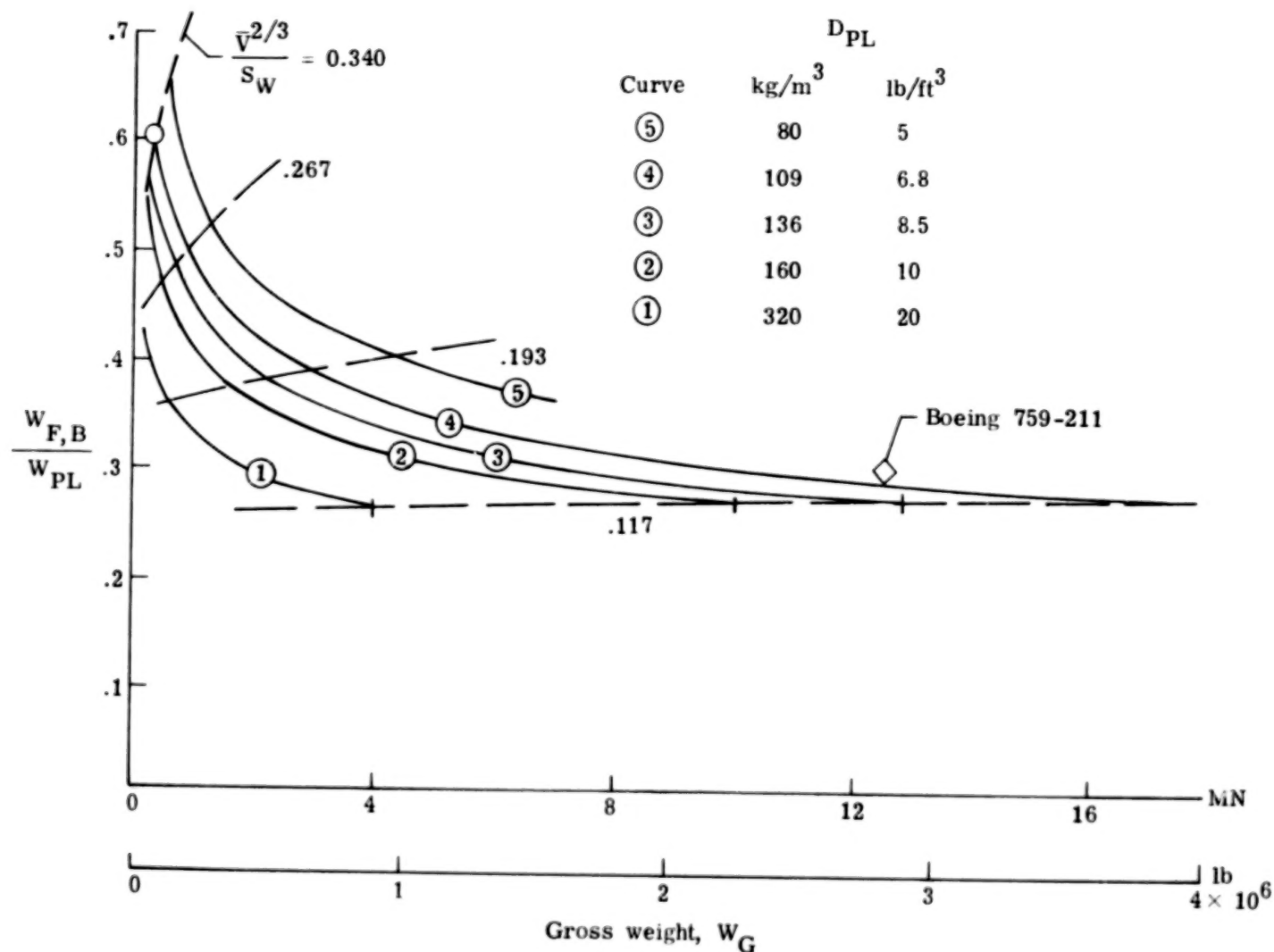
Figure 14.- Effect of wing loading and gross weight on block-fuel ratio. Payload in body and wing; K_{LD} varies; S_T/S_W varies; scaling laws from semiempirical column of table II but with wing weight defined by general equation of appendix.

43
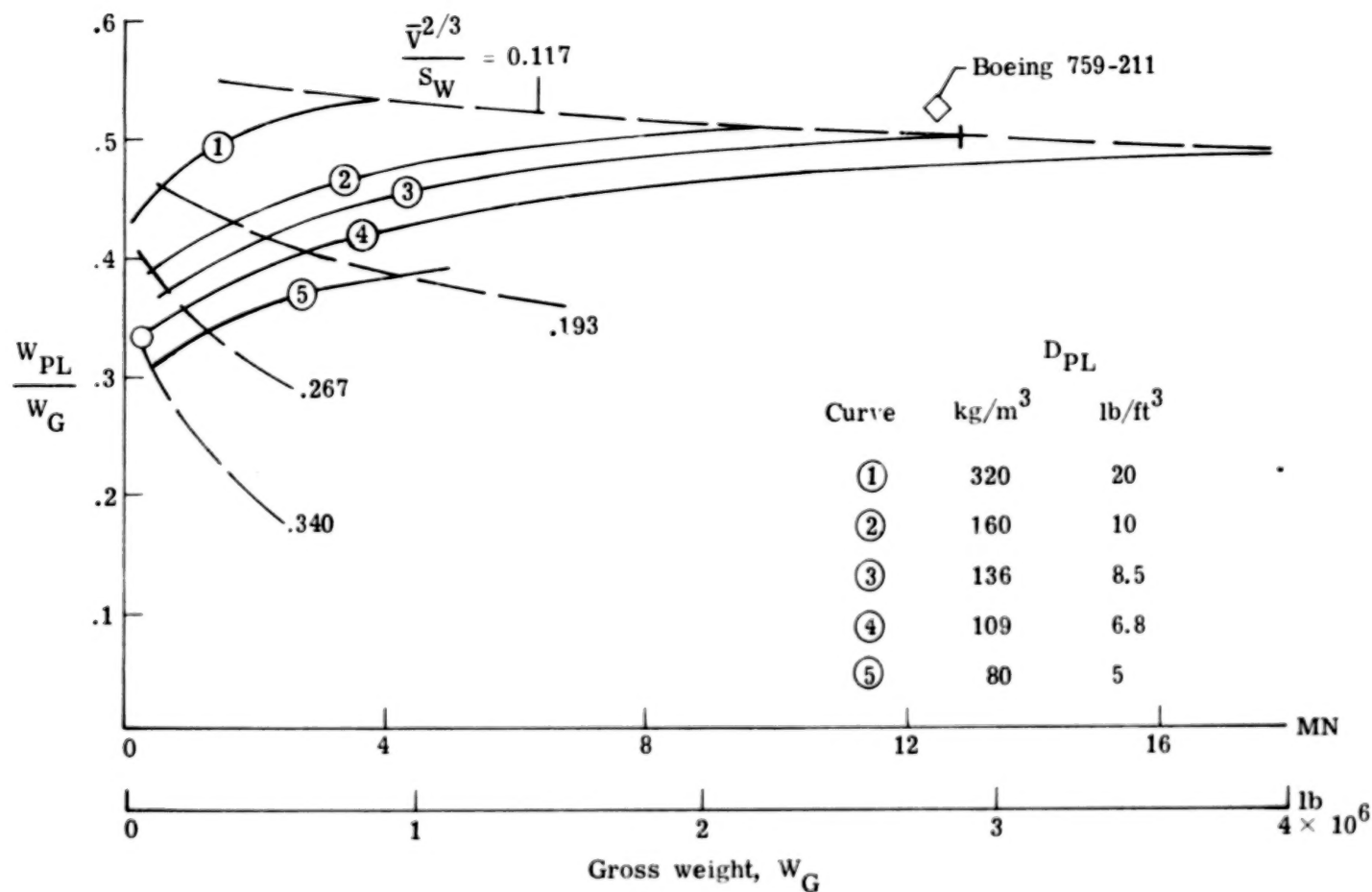
Figure 15.- Payload-ratio characteristics with $W_G/S_W = 3352$ N/m^2 (70 lb/ft^2); payload in body and wing; K_{LD} varies; S_T/S_W varies; scaling laws from semiempirical column of table II but with wing weight defined by general equation of appendix.

Figure 16.- Block-fuel-ratio characteristics with $W_G/S_W = 3352$ N/m^2 (70 lb/ft^2). Payload in body and wing; K_{LD} varies; S_T/S_W varies; scaling laws from semiempirical column of table II but with wing weight defined by general equation of appendix.

45
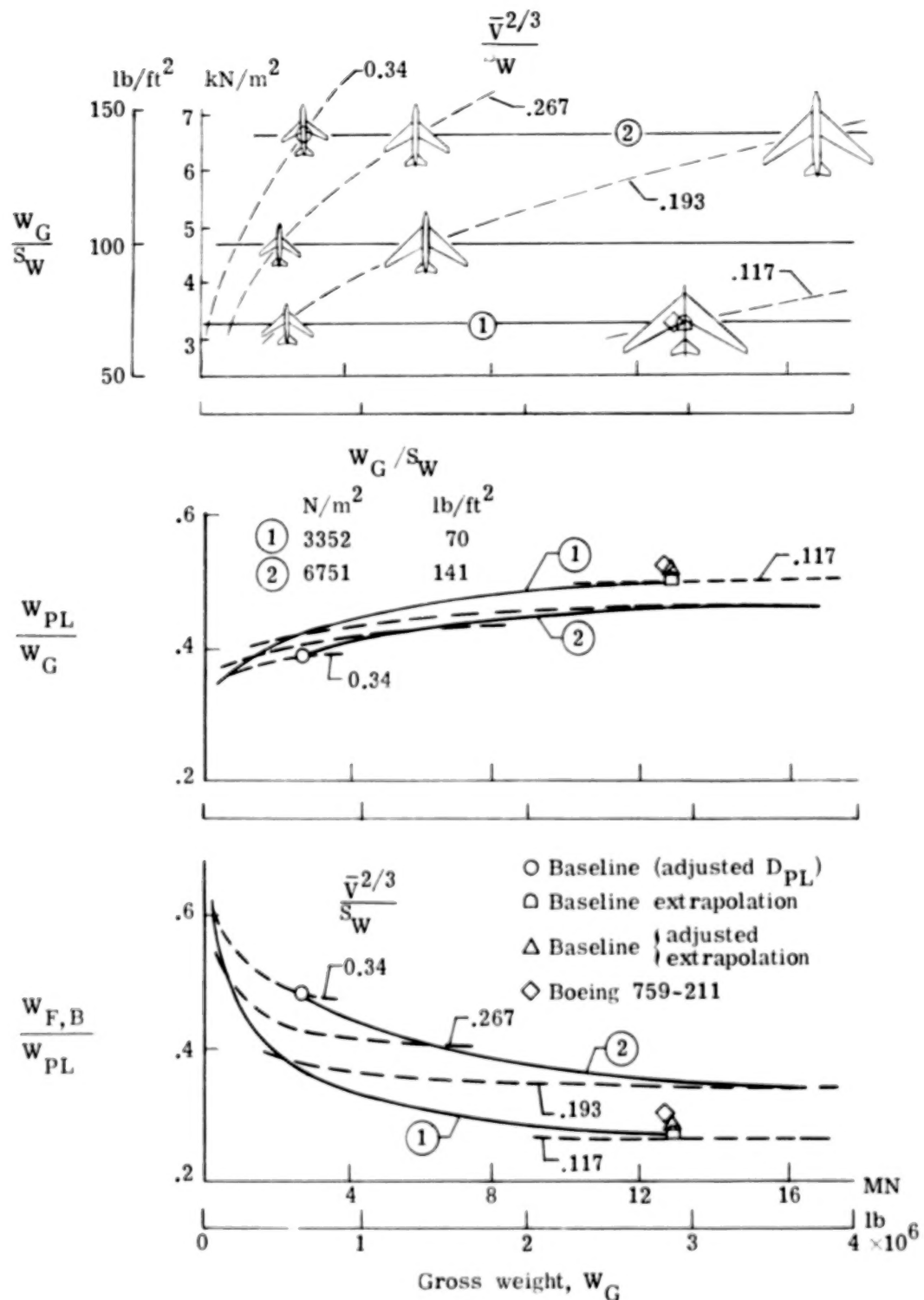
Figure 17.- Scaled variations with gross weight of payload ratio and block-fuel ratio, and corresponding relations to W_G/S_W and $\overline{V}^{2/3}/S_W$. $D_{PL} = 136$ kg/m^3 (8.5 lb/ft^3).
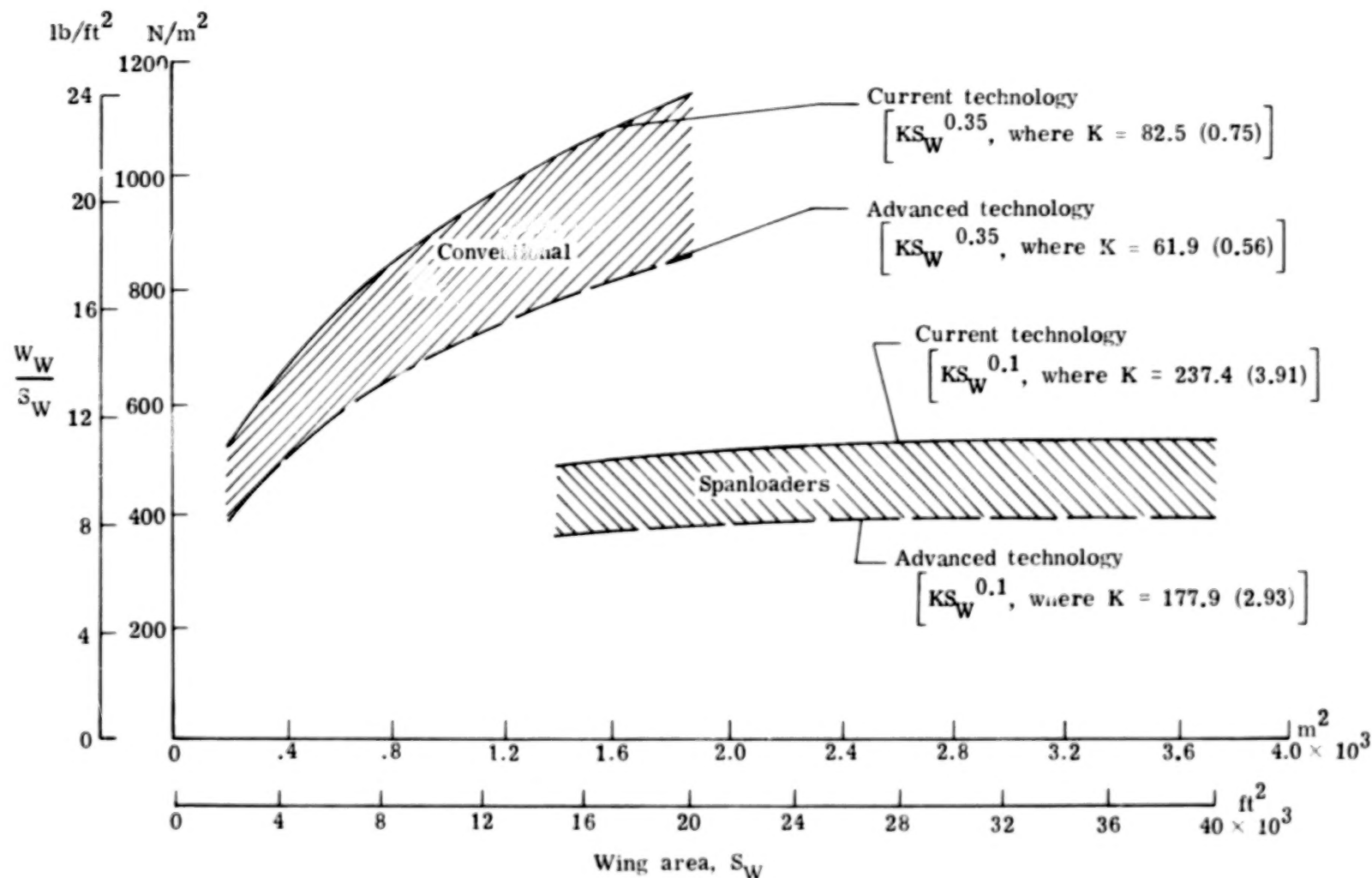
Figure A1.- Simple exponential wing-weight scaling relations as determined from correlations of data from current aircraft and from advanced aircraft studies.
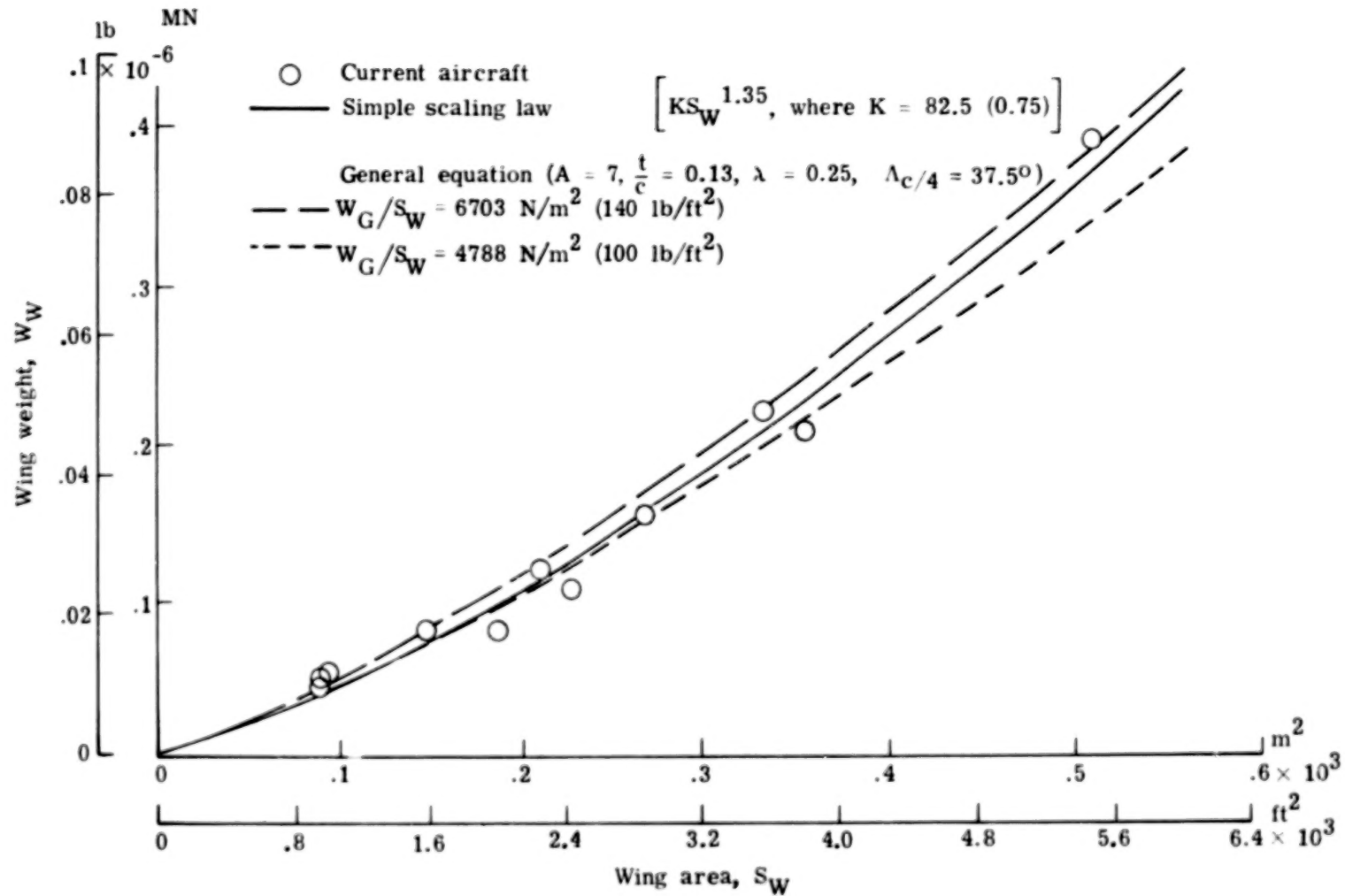
Figure A2.- Comparison of wing-weight data from current conventional transport aircraft
with results indicated by simple exponential scaling relation and by general wing-
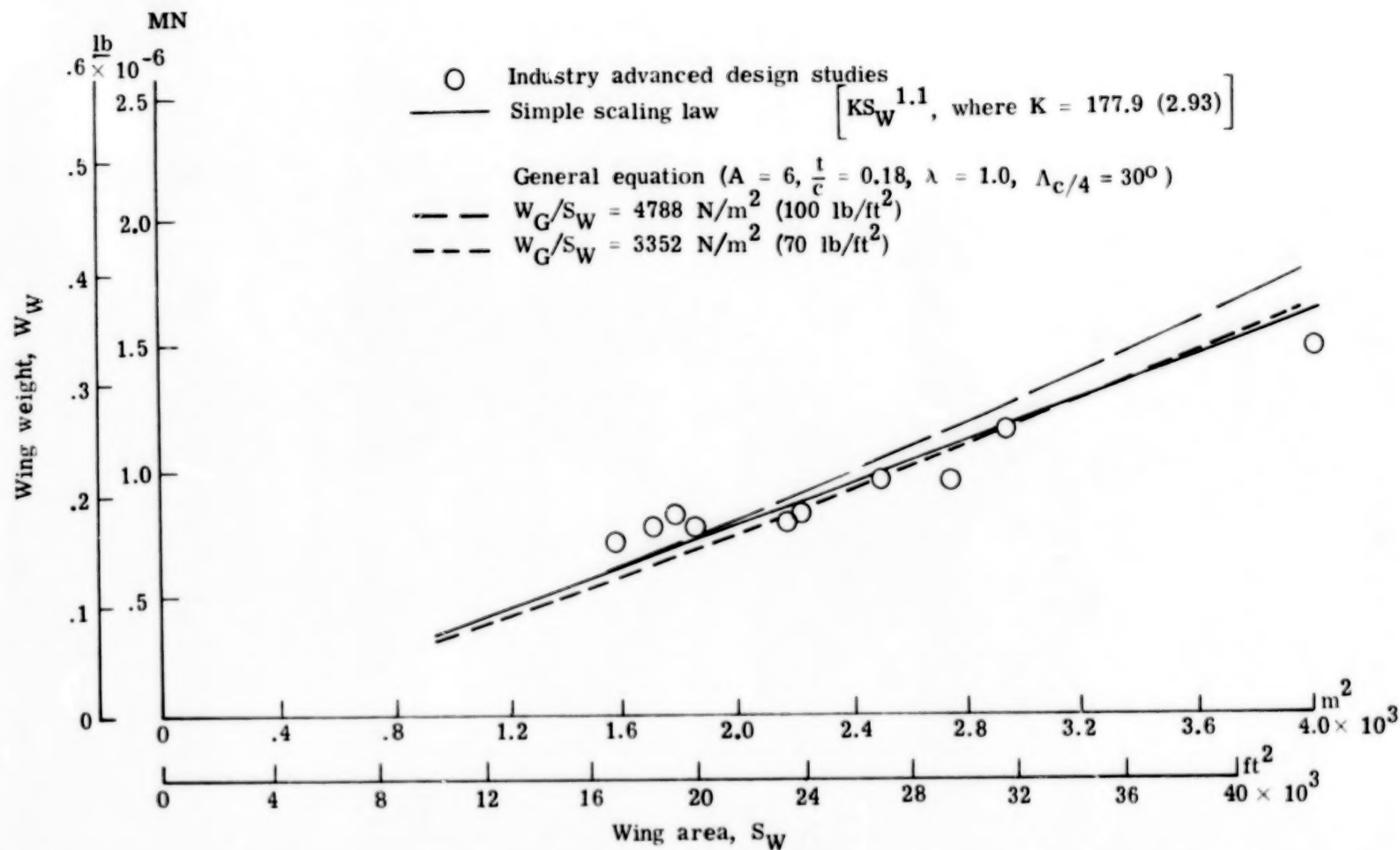weight equation.

Figure A3.- Comparison of wing-weight data from advanced spanloader studies with results
indicated by simple exporential scaling relation and by general wing-weight equation.
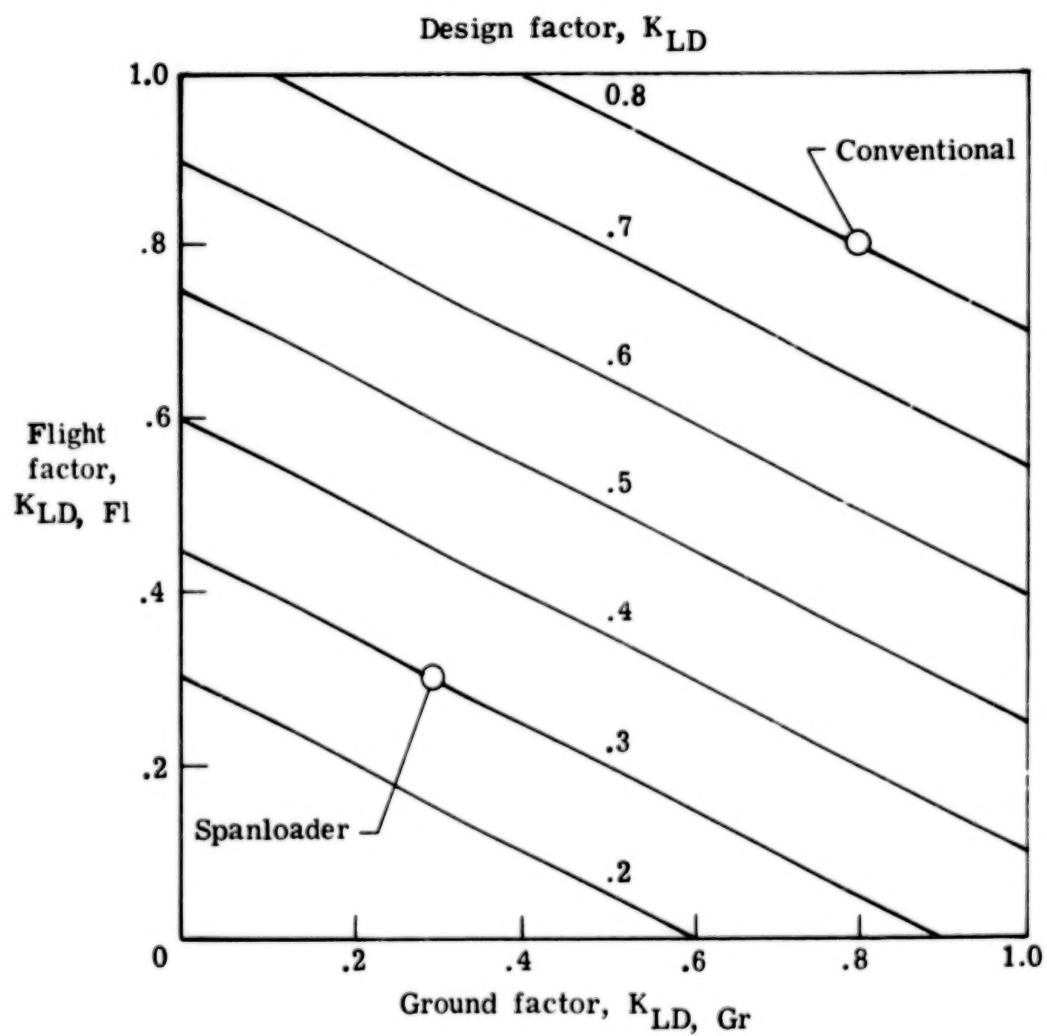
49

Figure A4.- Chart for estimating load-distribution-relief factor.

1. Report No. NASA TP-1625	2. Government Accession No.	3. Recipient's Catalog No.
4. Title and Subtitle PARAMETRIC STUDY OF VARIATION IN CARGO-AIRPLANE PERFORMANCE RELATED TO PROGRESSION FROM CURRENT TO SPANLOADER DESIGNS		5. Report Date April 1980
		6. Performing Organization Code
7. Author(s) Thomas A. Toll		8. Performing Organization Report No. L-13208
9. Performing Organization Name and Address NASA Langley Research Center Hampton, VA 23665		10. Work Unit No. 530-03-13-02
		11. Contract or Grant No.
12. Sponsoring Agency Name and Address National Aeronautics and Space Administration Washington, DC 20546		13. Type of Report and Period Covered Technical Paper
		14. Sponsoring Agency Code

15. Supplementary Notes

16. Abstract

A parametric analysis has been made to investigate the relationship between current cargo airplanes and possible future designs that may differ greatly in both size and configuration. The method makes use of empirical scaling laws developed from statistical studies of data from current and advanced-study airplanes and, in addition, accounts for payload density, effects of span-distributed load, and variations in tail-area ratio. The method is believed to be particularly useful for exploratory studies of design and technology options for large airplanes.

The analysis predicts somewhat more favorable variations of the ratios of payload to gross weight and block fuel to payload as the airplane size is increased than has been generally understood from interpretations of the cube-square law. In terms of these same ratios, large all-wing (spanloader) designs show an advantage over wing-fuselage designs; however, the comparison could be modified by other considerations.

17. Key Words (Suggested by Author(s)) Airplane performance Design Size effects	18. Distribution Statement Unclassified – Unlimited Subject Category 05
19. Security Classif. (of this report) Unclassified	20. Security Classif. (of this page) Unclassified	21. No. of Pages 50	22. Price* $4.50